Energy & Environmental Science

ROYAL SOCIETY OF CHEMISTRY

PERSPECTIVE

View Article Online
View Journal | View Issue

Cite this: *Energy Environ. Sci.*, 2026, **19**, 2507

Advanced pathways for hydrogen production: a collective view from a technical experts meeting

Katherine J. Chou,*[a] Yaset Acevedo,[b] Peter Agbo,[c] Alicia Bayon,[d] Alexander S. Beliaev,[e] Haluk Beyenal,[f] Trevor Croft,[a] Amgad Elgowainy,[g] Daniel V. Esposito,[h] Christoph Falter,[i] David S. Ginley,[j] Sophia Haussener,[k] Shu Hu,[lm] Erik Koepf,[n] Dhananjay Kumar,[o] Alon Lidor,[p] Bruce E. Logan,[q] Peter Loutzenhiser,[r] Anurag S. Mandalika,[s] PinChing Maness,[a] Gerald J. Meyer,[t] Graham J. Nathan,[u] Ruggero Rossi,[v] Ellen B. Stechel,[wx] Eric R. Sundstrom,[y] Emily Warren,[j] Lynn M. Wendt,[z] CX Xiang,[aa] Anthony H. McDaniel*[ab] and Frances A. Houle*[c]

Received 5th August 2025,
Accepted 24th November 2025

DOI: 10.1039/d5ee04503g

rsc.li/ees

Hydrogen is an essential fuel and feedstock that can be produced in multiple ways to meet requirements for technological sectors that include energy storage, transportation, petroleum refining, and ammonia synthesis. To consider the future state of hydrogen manufacturing, a team of experts has assembled and examined three emerging hydrogen production technologies – photoelectrochemical, biological, and thermochemical. Each of these emerging technologies holds significant long-term potential for cost reduction while lowering industrial emissions associated with conventional methods of hydrogen manufacture (*e.g.*, steam methane reforming) by using sunlight and renewable resources as primary sources of energy and feedstock, respectively. All three are currently at low technology readiness levels, however their applications, cost reduction opportunities and performance improvement pathways are under active development. In this work, opportunities and outlook for research that can directly advance the technologies are discussed.

[a] *Biosciences Center, National Laboratory of the Rockies, Golden, CO 80401, USA. E-mail: katherine.chou@nlr.gov, amcdani1000@gmail.com*
[b] *Strategic Analysis, Inc., 4075 Wilson Blvd, Suite 200, Arlington, VA 22203, USA*
[c] *Lawrence Berkeley National Laboratory, Chemical Sciences Division, 1 Cyclotron Road, Berkeley, CA 94720, USA. E-mail: fahoule@lbl.gov*
[d] *Instituto de Catálisis y Petroleoquímica (ICP), CSIC, Calle de Marie Curie, 2, Madrid, 28049, Spain*
[e] *Pacific Northwest National Laboratory, Richland, WA 99354, USA*
[f] *Voiland College of Engineering and Architecture, Washington State University, Pullman, WA 99164, USA*
[g] *Argonne National Laboratory, Argonne, IL 60439, USA*
[h] *Department of Chemical Engineering, Columbia University, New York, NY 10027, USA*
[i] *Synhelion AG, Dufourstrasse 101, 8008 Zurich, Switzerland*
[j] *Materials, Chemical, and Computational Science Directorate, National Laboratory of the Rockies, Golden, CO 80401, USA*
[k] *Laboratory of Renewable Energy Science, EPFL, 1015 Lausanne, Switzerland*
[l] *Department of Chemical and Environmental Engineering, School of Engineering and Applied Sciences, Yale University, New Haven, CT 06520, USA*
[m] *Energy Sciences Institute, West Haven, CT 06516, USA*
[n] *DuPont Silicon Valley Technology Center, Sunnyvale, CA 94085, USA*
[o] *Department of Mechanical Engineering, North Carolina Agricultural and Technical State University, Greensboro, NC 27411, USA*
[p] *Energy Conversion and Storage Systems Center, National Laboratory of the Rockies, Golden, CO 80401, USA*
[q] *Department of Civil & Environmental Engineering, Pennsylvania State University, University Park, PA 16802, USA*
[r] *George W. Woodruff School of Mechanical Engineering, Georgia Institute of Technology, Atlanta, Georgia 30332-0405, USA*
[s] *Center for Energy Studies, Louisiana State University, Baton Rouge, LA 70803, USA*
[t] *Department of Chemistry, University of North Carolina at Chapel Hill, Chapel Hill, NC 27599, USA*
[u] *School of Electrical and Mechanical Engineering, The University of Adelaide, Adelaide, SA, 5005, Australia*
[v] *Department of Environmental Health and Engineering, Johns Hopkins University, Baltimore, MD 21210, USA*
[w] *School of Molecular Sciences Arizona State University, Tempe, AZ 85287, USA*
[x] *ASU LightWorks®, Arizona State University, Tempe, AZ 85287, USA*
[y] *Advanced Biofuel and Bioproducts Process Development Unit, Lawrence Berkeley National Laboratory, Emeryville, CA 94608, USA*
[z] *Idaho National Laboratory, Idaho Falls, ID 83415, USA*
[aa] *Department of Applied Physics and Materials Science, California Institute of Technology, Pasadena, CA 91125, USA*
[ab] *Sandia National Laboratories, Livermore, CA 94550, USA*

Broader context

Hydrogen is both a commodity chemical and a fuel, where it offers an important alternative to carbon-based energy carriers. A variety of technologies can supply hydrogen at scale today, however advanced pathways – solar photoelectrochemical, biological, and solar thermochemical – are under development as long-term options that offer low pollution, low cost, and readily deployable alternatives. This article reports the outcomes of a meeting in which the three pathways were considered together, allowing their current state of the art and major technical opportunities and challenges to be compared. It is clear that there is no single pathway that is a best solution, rather the three present a suite of options for sustainable hydrogen generation that can be matched to diverse applications and geographic locations. Through their complementarity, the pathways provide future diversification and resilience to hydrogen production technologies. By advancing all three in parallel, there are significant opportunities for progress to be made through cross-cutting research and development that addresses challenges common to all.

1. Introduction

Hydrogen (H_2) is recognized as a commodity chemical used as a feedstock in petroleum refining, as well as in the production of widely used chemicals like ammonia and methanol. Its potential use as a long-duration energy storage medium and a dispatchable energy carrier are also well documented,[1,2] due to the availability of wide-ranging conversion technologies that can either produce or utilize it for heat and/or electricity. A case for expanding the use of H_2 into non-traditional sectors like metal ore refining, synthetic fuel production for aviation, and transportation is the foundational vision of the United States (U.S.) Department of Energy's (DOE) H2@Scale framework (shown schematically in Fig. 1), where its "consumption potential" in the U.S. could exceed 100 Mtonne year^{-1} in the absence of economic factors – effectively increasing H_2's market utilization 10 fold above 2015 levels while reducing industrial emissions.[3]

The current landscape for H_2 production predominantly relies on thermochemical processing of natural gas and coal, with steam methane reforming accounting for approximately 62% of this production globally in 2023[4] and the remaining balance up to 95% of global H_2 production derived from coal. And while finite fossil reserves are adequate to meet foreseeable demand, it is unclear how H_2 production capacity and chemical supply chains that are deeply integrated with petroleum refining and ammonia manufacture in the U.S. will adapt to a significant increase in demand from non-traditional end use. Critically missing is the necessary infrastructure required to transport H_2 to far-away end points for utilization. To realize H2@Scale, a diverse and flexible energy generation portfolio as feedstocks for hydrogen generation is needed. Such a portfolio will improve energy security and access to affordable energy across various regions within the U.S. Production costs from these various domestic resources need to be $<\$2$ kg^{-1} H_2 in order to stimulate the demand envisioned by H2@Scale.[3]

Currently water electrolysis powered by grid-electricity is the leading alternative to traditional methane- and coal-based hydrogen production routes. Electrolysis is commercial or near commercial depending on technology type, be it a low- or high-temperature processing platform, and will be important to the near-term realization of H2@Scale even though costs at this time are greater than \$6 kg^{-1} H_2.[5] However, future gigawatt-scale electrolyzer facilities powered by renewable electricity will require a significant expansion of renewable electricity generation and transmission infrastructure, as well as affordable energy storage technology, to achieve the high capacity factors and availability of low cost electricity needed to realize a $<\$2$ kg^{-1} H_2 price target. Concurrently, as the world continues to prioritize electrification of transportation and heating deemed necessary to achieve global emission reduction targets, the historically limited pace of renewable electricity deployments are better utilized powering these direct end-use needs as opposed to synthesizing fuels. In other words, the time required to achieve emission reduction targets is significantly shortened when direct end-use needs for electrification take precedence over fuel (*i.e.*, H_2) generation.[6] Furthermore, due to the complexity of manufacturing electrolyzer devices and support systems, this commercial enterprise may never achieve the 10's – 100's of MW scaled stack-sized facilities required to realize cost reductions necessary to reach $<\$2$ kg^{-1} H_2 even if electricity prices drop below \$0.03 kWh^{-1}.[7] Therefore, as part of a longer-term vision, we consider advanced pathways for H_2 production that require little or no electricity input and also leverage the nation's diverse renewable resources and feedstocks. The two most promising renewable domestic resources capable of meeting future H2@Scale hydrogen demand are solar[3] and biomass.[8]

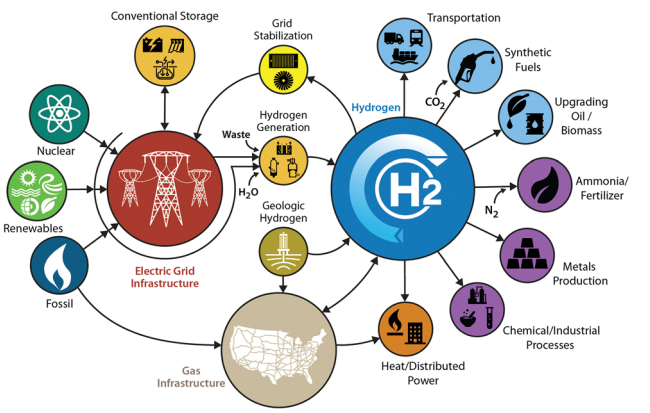

Fig. 1 Schematic of the H2@Scale hydrogen energy-centric ecosystem highlighting the production and utilization of H_2 as a primary energy carrier (see ref. 2).

1.1. Advanced hydrogen producing pathways

DOE's hydrogen production subprogram is actively developing three advanced pathways for renewable hydrogen production, each at relatively early stages of development but with significant potential for regional deployment as they mature. These pathways are Photoelectrochemical (PEC), Biological Hydrogen ($BioH_2$), and Thermochemical Hydrogen (TCH) – shown schematically in Fig. 2.

PEC hydrogen pathway. A low to moderate temperature process that bypasses the need for electricity by directly utilizing sunlight to split water into hydrogen and oxygen. This process relies on semiconductor photoelectrodes and/or particle-based photocatalysts to harvest light, separate charges, and promote water splitting.

Biological hydrogen pathway. A recent focus is on production of hydrogen by microorganisms from water and direct fermentation of biomass or organic waste streams, which is integrated with microbial electrolysis cells where microbial breakdown and oxidation of organic matter produces an electrical current to generate hydrogen with the application of a small voltage.

TCH hydrogen pathway. A moderate to high temperature process that can utilize renewable thermal energy sources to drive closed reaction cycles that net water splitting. Reaction networks can be simple two-step metal oxide cycles shown in Fig. 2,[9] or more complex schemes that involve the oxidation and reduction of multiple chemical species within the closed cycle.

1.2. Technology performance barriers and challenges

Overall, these advanced pathways represent promising long-term options, with continued research, development and demonstration (RD&D) required to address technical challenges and enable their transition from lab-scale demonstrations to commercial-scale deployment that meets H2@Scale goals. Improvements for all technologies are needed in cost, durability, efficiency, sustainability, manufacturing, and safety. These barriers and overcoming associated challenges will be a focal point of discussion in this perspective.

1.3. Technical experts meeting

In April of 2024, a Technical Experts Meeting (TEM) brought together 34 participants from academia, industry, and national research institutes from around the world. These individuals are recognized as global leaders in their respective fields, dedicated to advancing RD&D of these pathways for renewable and sustainable hydrogen production. This group was charged with assessing the current status of the aforementioned emerging H_2 production technologies, identifying RD&D gaps, and exploring the scientific and technical challenges that may impede their implementation. The TEM also identified opportunities for the research community to address – both fundamental science and engineering challenges – crucial to achieve the H2@Scale vision before mid-century. Participants were given questions in advance to stimulate discussion, and this manuscript is formatted to reproduce the structure and tone of the meeting, as well as capture collective thoughts and major outcomes.

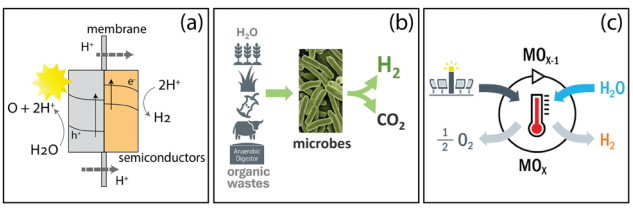

Fig. 2 Schematic of three advanced pathways. (a) photoelectrochemical (PEC); (b) biological ($BioH_2$); (c) thermochemical (TCH) Adapted with permission from the Electrochemical Society, ref. 9, Copyright 2021. Technology details are given in the text.

2. Photoelectrochemical hydrogen pathway

Examination of the status of the PEC advanced pathway centers on short- and long-term technology options, as well as on the scientific and engineering challenges that must be solved. The findings are summarized in this section. A variety of individual device and system architectures for PEC H_2 have been described in the literature, falling into one of three main types: wired photovoltaic-driven electrolyzers (PV-E), integrated photoelectrochemical systems (IPEC) which are assembled as a monolith with or without connecting wires and operate with either unconcentrated or concentrated sunlight, and photocatalytic particle systems (PCP) contained in panel or baggie structures.[10–16] Fig. 3 shows example designs of several main types as well as solar concentrators that they can be used with.[14,17,18] The PV-E and IPEC systems can be operated either fully immersed in aqueous electrolyte or be vapor-fed using a

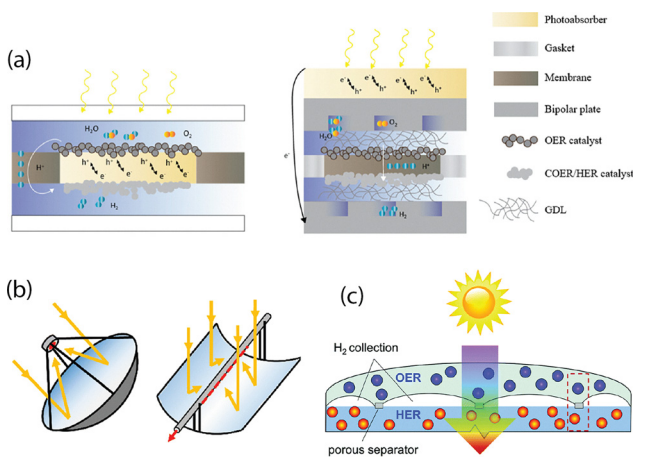

Fig. 3 Types of photoelectrochemical water splitting devices or systems that do not co-generate O_2 and H_2, so are intrinsically safe. (a) integrated PEC systems with liquid electrolyte (left) and gas diffusion electrodes in a PV-E configuration (right), adapted with permission from ref. 17, copyright 2024, The Authors; (b) solar concentrators for PEC systems, adapted with permission from ref. 18, copyright 2024, The Authors; (c) photocatalytic particle system with redox mediator connecting the vessels, Adapted from ref. 14, with permission from the Royal Society of Chemistry.

gas diffusion electrode (GDE). PCP systems are typically operated in liquid-phase aqueous electrolyte.

2.1. Current state of the art

2.1.1. Target metrics for PEC systems. Meeting the goal of $<\$2\ kg^{-1}$ H_2 will require the advancement of PEC water splitting devices towards the metrics shown in Table 1. Lifecycle assessments for at-scale installations of IPEC systems[19,20] have identified performance lifetimes of ~10 years with at most a loss of 80% of the original solar-to-hydrogen (STH)[21] conversion efficiency where a minimum STH of 10% is a requirement for positive energy return on energy invested for the lifespan of a full GW-scale facility using Si photocathodes coupled to WO_3 photoanodes.[20] Demonstration of pilot-scale systems (in the range of kW output power, or ~0.03 kg H_2 $hour^{-1}$)[22] that meet these targets and are constructed using inexpensive tandem photoabsorbers *e.g.* a cost of manufacture of \$30 m^{-2} for all-lead halide perovskite tandems *vs.* \$18 000 m^{-2} for III–V tandems[23] and highly active, robust water oxidation catalysts (<300 mV overpotential at 10 mA cm^{-2})[24] are needed to assess best-in-class designs. It is also essential that system designs ensure remanufacture and recyclability with minimal unwanted gas emissions and ecotoxicity over the system lifecycle.[18] The diversity of configurations shown in Fig. 3 brings with it many combinations of STH efficiency/lifetime/capital expenditure (CAPEX) that can allow for a final cost of $<\$2\ kg^{-1}$ H_2. For example, an analysis has shown that this cost can be met for STH efficiencies >7% and lifetimes of 1–4 years for particle systems having particle costs between \$105–1200 kg^{-1}. To reach this same cost target of $<\$2\ kg^{-1}$ H_2, an integrated PEC system using concentrated sunlight will require an STH of >40% and will have significant trade-offs between materials costs, lifetime, and concentration ratio.[25] A number of technoeconomic analyses (TEA) have been reported comparing PV-E systems to IPEC systems using diverse initial assumptions.[11,17,26–29] PV-E is currently closest to the final cost target at \$4–6 kg^{-1} H_2, while fully integrated PEC without solar concentration is about \$9–10 kg^{-1} H_2.

2.1.2. Today's benchmark system(s). Table 1 provides data on the current best performance metrics of IPEC and PCP technologies relative to the target metrics. While much of the literature focuses on photoelectrode (half-cell) improvements under continuous solar simulator illumination, there are important investigations of devices[30–32] and full systems operating under natural diurnal conditions.[22,33] A significant characteristic of each type of benchmark system is that they can be designed to operate at any scale with diverse applications ranging from standalone small- to large-scale installations serving large scale industrial end users or a hydrogen pipeline network.

Wired PV-E systems are the most mature type of PEC technology, and are most often based on Si PV cells.[35,36] These systems are not electrolyzers driven by solar panels, rather they use photocurrents generated directly by a photovoltaic element, often multijunction to improve photovoltage.[37] The most commonly explored electrolyzer designs for PV-E are polymer electrolyte membrane (PEM) electrolyzers based on membrane-electrode assemblies (MEAs) or alkaline electrolyzers. These are similar to conventional alkaline electrolyzers, for which the anode and cathode are fully immersed in an aqueous electrolyte and separated by a suitable ion exchange membrane or diaphragm divider. The highest performing PV-E system reported to date used high-efficiency III–V triple-junction solar cells operating with concentrated solar light (×42) wired to two series-connected polymer electrolyte membrane (PEM) electrolyzers using Pt and Ir catalysts to achieve high STH efficiency.[37] The light absorbers are electrochemically and thermally decoupled from electrolytes during water splitting. The 30% STH efficiency reported in that work is consistent with low cost target for H_2, and the operational stability shows a pathway to long-term on-sun diurnal operation. An assessment of whether this design could meet cost targets would be valuable. This system's efficiency outperforms others due to the coupling of the PV with two in-series electrolyzers that operate at low current density. The best performing PV-E system with Si-based solar cells achieves an initial STH efficiency of over 15%[35] and this would push the STH to over 30% if connected with two in-series ECs instead of one.[37] It should be noted that the 15% system is vapor-fed, simplifying the system and making it more cost-competitive.[17] Overall, the development of these systems as an advanced pathway solution will track improvements in electrolyzer technology[38] and PV technology.[39]

IPEC systems combine light absorption, charge separation, and electrochemical reactions in a single, integrated device to convert solar energy into chemical energy stored in H_2 and O_2 molecules. The light absorbers directly provide holes and

Table 1 Comparison of target metrics and state of the art metrics for full PEC systems

		PEC (all configurations)		Photocatalytic particle	
Parameter	Units	State of the art	Ultimate targets	State of the art	Ultimate targets
STH efficiency	%	5.5 (concentrated sunlight)[a]	25	1	10
H_2 production	kg day^{-1}	0.08[a]	10^5	0.7[b]	10^5
Degradation	% change in current per 1000 hours	<5[a]	2.5	20[c]	2.5
Useful lifetime[d]	years	0.3[a]	10	1300 hours	5
Cost	\$ $kg^{-1}H_2$	4–9[e]	<2	12	<2

[a] Ref. 22 system footprint 38.5 m^2, light collection area 142.4 cm^2, electrochemical area 50 cm^2. [b] Ref. 33 total panel area 100 m^2. [c] Ref. 34. [d] Ref. 20. [e] Ref. 17.

electrons with the potentials required for water oxidation and H_2 evolution, respectively.[12,40] In all cases an electrical junction is required to direct photogenerated holes toward the anodic interface and photogenerated electrons to the cathodic interface. This junction was originally conceived to be at the semiconductor–electrolyte interface;[41] however semiconductor photocorrosion led to integrated systems constructed using buried junctions and protection layers to separate the electrolyte from materials susceptible to such reactions.[42] As in the PV-E case, numerous types of GDE-type and fully aqueous systems have been reported. The component integration sometimes requires explicit electrical wiring. The PV-integrated Membrane (PIM) assembly is another scheme for realizing fully-integrated, PEC devices. In this case, multi-junction PV cells are embedded in a Nafion membrane,[43] with the membranes, catalysts, and PV cells integrated through direct ohmic contacts, resulting in a wireless, monolithic PEC assembly operating with vapor-fed water.[44]

Particle-based photocatalysts in aqueous electrolyte, usually in a colloidal suspension or immobilized on a panel in the form of a so-called ''photocatalytic sheet'' supported by a conducting substrate, offer the possibility of low-cost manufacture and assembly of scalable PEC reactors.[33,45–47] The particles perform light absorption, charge separation, charge trapping or accumulation, and catalysis (often in conjunction with an inorganic co-catalyst). Compared to a colloidal suspension, the photocatalytic sheet system is dense and facilitates multiscale transport of charge carriers and molecular species through the semiconductor/cocatalyst/liquid interface.

Unlike the PV-E and IPEC systems, where photogenerated charge-induced reactions are separated by micrometers to millimeters, the reduction and oxidation sites on particles are in nanoscale proximity and cannot easily be separated by membranes as in the other architectures. Specifically, if the photocatalysts are operated in a single chamber, they coevolve H_2 and O_2 which presents significant safety hazards.[48] However, redox-mediated water splitting, commonly referred to as ''Z-scheme water splitting'', can allow for intrinsically safe operation by coupling separated chambers containing two different types of photocatalysts (Fig. 3(c)).[14] In this scheme, H_2-evolving photocatalysts produce H_2 in one chamber while selectively oxidizing a redox shuttle. The oxidized shuttle diffuses to the second chamber where it is selectively reduced when the O_2-evolving catalysts produce O_2. An example of a shuttle are the I^- and IO_3^- mediators. The solar spectrum is split between the H_2-evolving and O_2-evolving photo-reactions if the chambers are placed on top of each other. For example, O_2-evolving photocatalysts absorb the solar light unused by the H_2-evolving photocatalysts. The top STH efficiencies for suspensions without a mediator are 0.65%, while the photocatalyst sheets[49] have achieved just above 1% STH efficiency with $BiVO_4$ and $SrTiO_3$:Rh photocatalysts.[14]

2.1.3. Cross-comparison considerations for system-level metrics. These benchmark systems have different time horizons due to their level of maturity. PV-E is the most straightforward to deploy in the short term because it combines established technologies that have already demonstrated high efficiency at large scale. In the long term, all three can be operated as standalone systems using sunlight as the sole source of energy, and further development is needed to evaluate which one will ultimately be the most successful. While these architectures are significantly different from each other, their performance can be compared in terms of STH efficiency, H_2 production rate, and degradation rates. Economic metrics to compare these systems include levelized cost of H_2 ($LCOH_2$), CAPEX or operating expenses (OPEX). TEA have examined these cost factors across system types, revealing that significant improvements are needed to make solar-driven technologies comparable to or less expensive than electrolyzers as discussed below.

Sustainability metrics to compare these systems include energy returned on energy invested (EREOI), greenhouse gas emissions and ecotoxicity.[18,50] Although there are fewer studies, EREOI for PV-E and IPEC installations is likely to be positive.[19,20,51] Social metrics to compare these systems include the potential to create jobs and the acceptance level of the technology itself. The importance of these has been recognized,[10] and they will be a focus as the technologies and their applications develop. Their scalability or manufacturability are equally important.[18,52] Notably, investments in these benchmark systems for H_2 production are a gateway to other solar-driven energy conversion chemistries, including light-driven CO_2 reduction,[53,54] N_2 or nitrate reduction,[55,56] and H_2O_2 synthesis.[57]

2.2. What does success look like for PEC technology?

Success for PEC technology hinges on achieving advances in scalability, systems engineering, large-scale deployment, and meeting ambitious performance targets related to efficiency and stability (Table 1). Additional environmental metrics such as carbon footprint, H_2 leakage rates, and water usage should also be tracked during scaling from prototype demonstrations to deployed pilots and commercial plants in order to optimize them. These elements collectively define the trajectory of PEC from its current low technology readiness level (TRL) to commercial hydrogen generation plants that are capable of addressing global hydrogen demands in a safe, cost-effective, and sustainable way. What exactly will success look like? While different types of PEC technology may be very different in appearance (Fig. 3), successful deployment of any of these technologies is very likely to have much in common (Fig. 4), resting on key performance indicators such as applied bias photon-to-current efficiency (ABPE), defined in ref. 21, eqn (9), lifetime[20] and apparent QY for photocatalytic systems, defined in ref. 58, eqn (5).

2.2.1. Scalable PEC reactor designs. A critical measure of success for any energy conversion technology is that it be deployed at production scales that allow it to achieve significant market share, and therefore impact. Achieving PEC deployment at large scales is also crucial for realizing economies of scale that will be necessary to drive down the $LCOH_2$ production, as has been the case for related technologies such as PEM

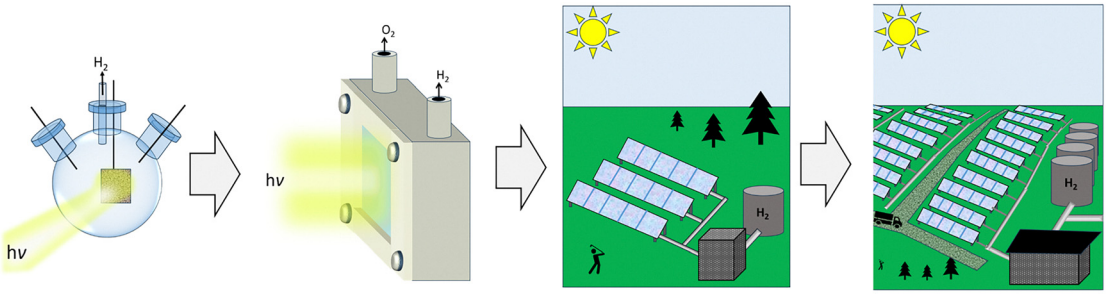

Key features	Benchmarking scale	Prototype scale	Pilot scale	Commercial Scale
Components	Single photoelectrode or particle type	Complete reactor without external bias	Fully integrated system including nearly all auxiliary unit operations	Full-scale system with all functionalities producing H_2 for customers
Technology readiness level (TRL)	1-2	4-6	7-8	9
H_2 production rate	0.1-10 mg/hr	0.01-100 g/day	1-1,000 kg/day	0.1-500 ton/day
Key performance indicators (KPI)	ABPE, QY, lifetime	STH efficiency, lifetime, purity	System STH efficiency, lifetime, purity	System STH efficiency, lifetime, purity, capacity factor

Fig. 4 Progression of PEC technology from materials development at benchmarking scale to commercial applications.

electrolyzers, fuel cells, and batteries.[59] Recognizing this, it is necessary to develop scalable PEC reactor and system designs that can be translated from small laboratory-scale prototypes (0.5 mg h^{-1}) to commercial scale plants (5–10 tonnes day^{-1}) that maintain or exceed the level of performance achieved at small scales. The World Energy Outlook 2024 "Stated Policies" case published by the International Energy Agency[60] projects a deployed capacity of 49 Mtonne $year^{-1}$ of low-emissions hydrogen production by 2030. Successful deployment of six 10 Mtonne $year^{-1}$ photocatalytic hydrogen production plants could capture 1.5% of the low-emissions H_2 market. As previously described,[16] scale-up in fuel production by PEC technologies can be achieved through one or more different approaches, including (1) increasing the size of individual reactor units, (2) increasing the number of modular reactor units, and/or (3) using optical concentration to increase the effective light harvesting area per module. In all cases, scaling must account for technical challenges such as multi-phase flow dynamics, thermal expansion and contraction uniformity, ohmic losses, and the ease with which the design can be manufactured and installed. To date, notable PEC demonstrations at scale have included a 100 m^2 demonstration based on photocatalytic sheet panels[33] and a ~2 kW concentrator PEC system.[22]

2.2.2. Optimized PEC systems. Although the majority of PEC-related RD&D activities focus on materials development and/or the design of PEC "devices" or reactors, it is important to recognize that the PEC reactor will only be one part of a system in which it must seamlessly integrate with auxiliary unit operations like pumps, compressors, deoxygenators, dryers, water purifiers, piping networks, trackers, sensors, storage tanks, and more.[17,28] Recognizing this, pilot plants that integrate the reactor with auxiliary units to form a system are pivotal in their roles of (1) derisking the technology and (2) bridging the gap between lab-scale reactor prototypes to commercial scale plants. Successful pilot plants will require integrated process control, ramp-up and ramp-down procedures, and the ability to produce hydrogen at purities and pressures suitable for downstream applications. Conversion losses associated with auxiliary units such as pumps and compressors must be considered when determining the systems-level STH efficiency. Durability tests within a pilot system are also an important step in the de-risking process, and must account for the fact that interactions between units can lead to perturbations in operating conditions that could result in component failure in cases where degradation would not have been an issue during well-controlled lab testing at the prototype stage. Ideally, a pilot-scale demonstration would achieve a target operational lifetime of 1000–10 000 hours.

2.2.3. Deployment in operational environment. Large-scale deployment would involve systems operating at gigawatt levels and enabling hydrogen production for diverse applications ranging from the manufacture of commodity chemicals like ammonia and methanol to grid-scale energy storage and off-grid mining operations in remote areas. While pilot demonstrations with access to the electrical grid may be useful for initial systems optimization and derisking efforts, it can be anticipated that off-grid deployment of PEC systems that can be available to a broad array of hard-to-serve regions needing H_2 but do not have reliable electricity or bypass additional regulations and constraints related to making and maintaining grid connections will lead to new markets and provide additional avenues for technology innovations. However, off-grid operation will also bring new challenges. For example, achieving

efficient and safe gas separation, handling, and storage under dynamic operational conditions (*e.g.*, diurnal cycles) may require advanced process control and/or careful design of back-up energy storage (*i.e.* batteries and PV panels). Another consideration is environmental factors that can be highly specific to a location of interest,[61] including but not limited to dealing with the mix of direct and indirect insolation, freezing conditions, extreme heat, source water purity, dust deposits, *etc.* Water quality requirements for PEC H_2 generation have not been deeply evaluated so far, however there are benefits to combining hydrogen production with water purification processes such as seawater desalination.[62] Efficiency, product purity and durability challenges are posed by chloride anions and metal cations when seawater is used as a feedstock and need to be mitigated, It is worth noting that even when the water feedstock is ultrapure, the salts added to support current flow and metals from corroding electrodes produce a non-ideal environment.[63]

2.2.4. Broader impact. Beyond technical success, PEC technology must deliver social, environmental, and economic benefits. Its modular, mobile, and grid-independent nature supports rapid deployment, especially in underserved or remote areas where the grid is unavailable. PEC systems also present opportunities for environmental remediation, including clean water generation and CO_2 capture. Furthermore, the development of PEC technology can drive workforce diversification, create jobs, and promote energy democratization through decentralized hydrogen production systems. However, addressing environmental impacts, such as the considerable amount of land use required when using unconcentrated sunlight to excite photoabsorbers that are inherently Schockley–Queisser limited ($<$30% STH efficiency), water use, and material sustainability, remains critical to ensuring long-term viability and public acceptance. Towards this end, it is essential that government agencies and companies encourage additional studies in the area of life cycle assessment (LCA) of PEC technologies, which have been very limited to date.[19,20]

2.3. Targets, barriers, and opportunities

2.3.1. Targets. As indicated in Table 1, reducing the cost of H_2 to $<\$2\ kg^{-1}$ requires significant advancements relative to the current state of the art. The state of PV-E development makes it likely that these types of devices will be the first to achieve the cost target. By comparison, the state-of-the-art in IPEC and particle devices and the challenges identified point to a longer time requirement.

2.3.2. Barriers. Meeting target metrics for all PEC technologies will require significant improvements in efficiency and useful lifetime using high performance but low-cost materials. A common challenge to all systems is the solar spectrum which spans infrared to ultraviolet wavelengths and can only be partially absorbed by semiconductors. Because of the magnitude of the photovoltages and currents required to drive the chemical reactions involved in hydrogen production at a useful rate, high performance photoabsorbers require both a balance of absorptivity of higher energy photons and sufficient mobility of the charge carriers formed by photoexcitation.[12] Barriers to progress originate from insufficient understanding of the factors that affect efficiency and lifetime, particularly for low-cost membranes, catalysts and light absorbers, a lack of good synthetic methods for high volume materials manufacturing, and limited experience with deployment of large-scale reactor and system designs that are intrinsically safe. Efficiency and lifetime improvements for PV-E systems will track progress in low temperature electrolyzer technologies.

Because of their operating environment, the most significant stability challenges in IPEC systems[64] are typically associated with semiconductor corrosion[65] and catalyst stability.[66,67] However, other instabilities may also be present, including mechanical damage from bubbles (cavitation),[68,69] thermal expansion, and membrane degradation in use.[70,71] Meeting the economic target of low-cost H_2 with current materials sets will require either developing (photo)electrochemical materials systems where high activity is achieved using low loadings of expensive catalysts based on noble metals (Pt, Ir, Ru) or inexpensive,[72] less active abundant ones (Fe, Co, Ni) at higher loadings, all on Si or other inexpensive visible light-absorbing PV materials such as oxide-based semiconductors or lead-halide perovskites. Regardless of the semiconductors used, a decrease in the overpotentials required by these catalysts is necessary to improve efficiency. Additionally, perovskite PV materials appear to be only practical for PV-E applications where the semiconductor material can be put in a rigorously controlled environment, for example separated from an aqueous environment. A transition to polyelectrolyte membranes that are rigorously stable in use and not perfluoro hydrocarbon-based is also important.[73] Accelerated timelines for realizing these improvements are key: they will be a major factor shaping IPEC technology adoption.

While demonstration projects have provided convincing arguments for particle systems, the relatively low efficiency and TRL of intrinsically safe (*i.e.* separated H_2 and O_2 production) PCP systems compared to the PV-E devices may pose a challenge for penetration into the clean hydrogen markets. A specific challenge that limits many PCP systems from achieving high efficiency is controlling redox selectivity in a way that promotes the desired water splitting or Z-scheme reactions while minimizing undesired back reactions that reduce STH efficiency.[14,74]

2.3.3. Opportunities. As the technology matures, the research community has the opportunity to address both fundamental science and engineering challenges of PEC systems. These challenges involve performance as well as those posed by scaleup of systems designs and fabrication methods required for cost-effective mass manufacturing of PEC components and devices as listed in Table 2. Each type of PEC system presents different opportunities. To illustrate this point we consider nearer term PV-E systems, and longer-term but perhaps cost-advantaged particle-based systems, and compare them to IPEC systems.

PV-E systems are capable of operating at high efficiencies and with lifetimes currently unmatched by IPEC systems or PCP systems. However, progress is still needed to demonstrate

Table 2 Improvements for PEC hydrogen pathways

	R&D Opportunities
PV-E and PEC designs	Testing of prototype scale demonstrators H_2 collection and transportation systems Use of waste heat to improve systems
Photocatalytic particle designs	High efficiency with full separation of O_2 and H_2
All systems: catalysis and photocatalysis	Efficiency of the oxygen evolution reaction
All systems: durability	Degradation-resistant materials
All systems: low cost manufacturing	Fabrication of high performance reactors using low cost materials and processes

scalable manufacturing, efficiency, and stability. Module demonstrations need to take place at a physical scale that can address balance of systems (BOS) integration in a realistic way (gas/liquid transport and separation, packaging, material uniformity) so that BOS infrastructure engineering can maximize STH efficiencies. These demonstrations should be on the order of 10–100 m^2 of active panel area to test the viability and actual costs of system designs. Based on designs from the PV industry, the panels are most likely to be modular, constructed from cells of about 100–1000 cm^2 tiled within the water and product gas handling infrastructure.

Particle systems have been shown to be attractive from high level technoeconomic studies.[11] While concepts for the intrinsically safe designs[14] have been explored[45] they have yet to be realized in fully scaled systems. InGaP nanowires have achieved 9% STH efficiency for 74 hours with subsequent performance loss attributed to catalyst dissolution.[75] Al-doped $SrTiO_3$ photocatalyst particles, on the other hand, were determined to be stable for 1300 h with an STH of 0.3%.[34] Demonstrating systems with STH efficiencies greater than 2% with stability in the range of 1000's of hours and full H_2 and O_2 separation within the reactor would be an advancement in the field. Materials and design improvements and understanding how durability and corrosion impact particle-based systems are all possible areas of development.

Beyond these PV-E and particle-based systems considerations, breakthroughs in catalysis and photocatalysis are also needed for all technologies. In particular, improving the activity of oxygen evolution catalysts using novel, stable materials and enhanced charge separation of photogenerated charge carriers will have a large impact on performance. Transition metal oxides offer an avenue to bandgap engineering *via* metal or N doping for high performance multijunction photoelectrodes and particle-based technologies as well as providing a platform that is more stable to photocorrosion than Si and III-V semiconductors.[76] The efficiency of photocatalytic oxygen evolution reaction can be enhanced using a built-in electric field present in semiconductor-based heterojunctions to direct flow of electrons away from the active surface and holes toward it.[77] Additionally, oxides can have reduced overpotential for water oxidation such as found for TiNO films, where the overpotential is as low as 290 mV at 10 mA cm^{-2}, the current density typical of light-driven water oxidation systems.[78] A scalable production of this material will require roll-to-roll or rapid sputter deposition, presenting additional materials synthesis innovation opportunities that may be useful for manufacturing other oxides. While water oxidation is currently the central chemistry for large scale H_2 production, pursuing other photooxidation chemistries such as glycerol oxidation which operate at a lower overpotential may offer a better path toward efficiency although the achievable scale may be limited.[79,80] Improvements are also needed in understanding carrier collection/accumulation, and charge transfer phenomena (including photocorrosion) in particle systems, especially at low light flux/low current densities relevant to these systems.

Unlike PV-E devices, which have physically separated light absorbers and electrolyzers, IPEC and PCP devices share opportunities for using thermal management to improve device performance.[18,81,82] Electrolytes may serve as heat sinks, by both thermal energy transfer from the illuminated photoabsorber and directly absorbing low energy photons. The resulting electrolyte temperature increase can be used to increase the catalyst turnover frequency, particularly for catalytic water oxidation where the intrinsic kinetic barriers are often rate limiting.[83] Operation at elevated temperature has also been shown to be advantageous for PCP systems.[75,84] Recent work on faceted N-doped TiO_2 photocatalyst particles[84] reported STH efficiencies up to 20% and overall efficiencies up to ~16% for operation in electrolyte-containing solutions at elevated temperature (150–270 °C) and pressure. Such possibilities for exploiting kinetic and thermodynamic advantages of operating at elevated temperature will become increasingly salient as work on solar-concentrated hydrogen evolution and water oxidation advances.

Advances in scientific understanding will directly inform progress in engineering. Recent TEA studies have examined in detail the costs associated with manufacturing H_2 using PEC systems and point the way to removing economic barriers.[17,28,85] The studies have considered full plants at the 610 tonne day^{-1} (ref. 28) and 1 tonne day^{-1} (ref. 17) levels, and have reached comparable conclusions on cost drivers. These are the cost of the modules, including the materials in the PEC reactor, their size, and their lifetime (replacement frequency). A comprehensive TEA[85] prepared for this report for panel and particle-based systems is presented in Fig. 5, putting the module cost in context with land and operating costs. Land requirements are proportional to module efficiency, so will be reduced as efficiency is improved.

To measure progress toward meeting target metrics, it is essential to develop best practices and protocols for testing and benchmarking the efficiency and reliability of PEC systems.[52,86–90] To be relevant to meeting the <\$2 kg^{-1} goals, initial tests should target accelerated and "real world" operational tests to demonstrate performance in the range of 1000 hours initially, and building up to multi-year operation. This includes understanding at a fundamental level any changes during day/night cycles and seasonal variations in insolation and environmental conditions. These new practices will support certification to enable robust comparison of H_2 production across technologies.

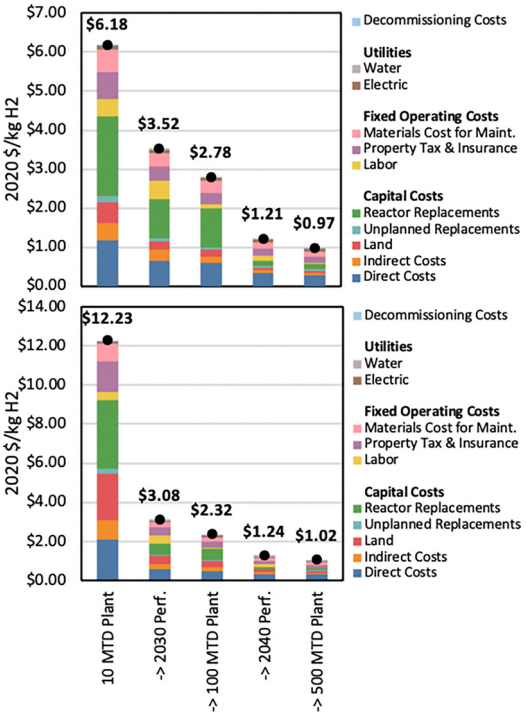

Fig. 5 TEA data for two types of plants, panel-based (top) and particle-based (bottom). The trends illustrate the impacts of scaling and technology improvements, with targets as listed in Table 1. It is evident that decreases in land and capital costs are connected to increases in system efficiency.

3. Biological hydrogen pathway

Biohydrogen ($BioH_2$) is H_2 produced from water molecules *via* microbially catalyzed, light-driven reactions[91–95] (also known as solar H_2) as well as from biogenic materials (*e.g.*, plant biomass, lignocellulose, wastewater, farm/animal waste, *etc.*) through fermentative catabolism without light input. Conversion of these starting feedstocks can be achieved through biological,[96–99] thermochemical,[100,101] bio-electrochemical,[102,103] or hybrid technologies (SI Fig. S1).[104–106] This emerging definition of $BioH_2$ encompasses a broader scope of conversion methods and contrasts with earlier literature which limited the term $BioH_2$ to H_2 produced biologically by microorganisms.[107,108]

3.1. Current state of the art

H_2 production through microbial dark fermentation (DF) of lignocellulosic biomass emerged as one compelling biological approach owing to fast microbial growth rate and H_2 productivities. Hybrid systems integrating biological, thermochemical, and electrochemical mechanisms to produce H_2 are also considered. Microbial electrolysis cells (MEC) are a hybrid technology that couples the oxidation of organic matter in liquid wastes with electrochemical H_2 generation, enabling gas production while removing organic contaminants from domestic and industrial wastewaters.[109–113] H_2 can also be produced from reforming biogas generated from anaerobic digestion (AD) of heterogeneous, organic wastes.[106] Compared with PEC and TCH pathways, H_2 production *via* dark fermentation, MEC and AD are independent of solar energy but rely on organic materials as the feedstock. $BioH_2$ is produced as organic waste streams are remediated, which represents a unique benefit of this technology. Compared to abiotic approaches which may require high purity feedstock, complex and variable media/feed streams can be utilized by leveraging the selectivity of biological reactions therefore minimizing costs.

Several microbial $BioH_2$ production pathways have been intensely studied historically, including biophotolysis, photo-fermentation (PF), and dark fermentation (DF).[109–113] However, the focus of the discussions was on dark-fermentation integrated with microbial electrolysis cell as dark fermentation generally due to the relatively fast hydrogen production rates compared with biophotolysis and photo-fermentation.

3.1.1. Today's benchmark systems. One system that contends to reaching economic feasibility integrates DF with MEC (Fig. 6), and such coupling of DF and MEC is designed to increase H_2 recovery toward the theoretical maximum amount of H_2 per sugar (*i.e.*, glucose) that constitutes biomass. Fermentation occurs in the dark and is therefore not affected by the intermittency of sunlight. Fermenting microbes are robust catalysts with key hydrogenase metalloenzymes catalyzing H_2 production without using expensive precious metals. Microbes can utilize diverse feedstock including organics in waste streams as well as the abundant and renewable lignocellulosic biomass afforded by cellulose- and hemicellulose-degrading microbes.[114] While acetate is the most common fermentation byproduct of DF, fermentation also produces a variety of other organic acids and alcohols, including lactate, butyrate, and ethanol, among others.[115,116] When integrating DF with MEC, most of these fermentation byproducts can be completely oxidized to CO_2 in the MEC, generating additional H_2. This process results in higher H_2 molar yields (mol H_2 mol^{-1} substrate) while producing an effluent with reduced organic matter concentration. A combined H_2 molar yield (per mole of

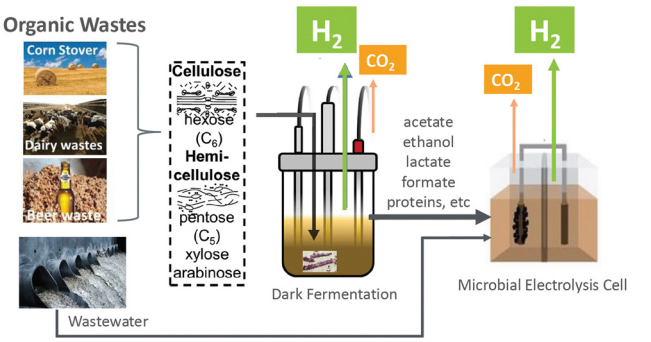

Fig. 6 Overall scheme of dark fermentation (DF) integrated with microbial electrolysis cell (MEC). Lignocellulosic biomass can be hydrolyzed (solubilized) and the sugars embedded in the biomass are utilized for hydrogen production during DF. The fermentation wastewater containing residual organic acids as well as other aqueous waste streams can be fed to the MEC for additional hydrogen production. The CO_2 produced during hydrogen generation originates from the atmospheric CO_2 fixed into the biomass. H_2 and CO_2 are two main gaseous products that can be separated *via* pressure swing adsorption.

the sugar that makes up the biomass) of ~10 has been demonstrated from cellobiose fermentation in an integrated DF-MEC system,[104] compared to only 4 from DF alone, showcasing its immense potential and warranting further investigation.

3.1.2. Cost drivers. High H_2 yield, productivity as well as the durability of each component within the DF-MEC system must be achieved with low capital and operating expenses. The key cost drivers for $BioH_2$ production using this integrated approach are the capital costs associated with materials and equipment (*i.e.*, bioreactor, feedstock, cathode/anode/membrane, *etc.*), followed by the amount of electricity used and its cost (mainly concerns MEC), as well as the fixed operating and maintenance (O&M, aka OPEX) cost (Fig. 7a). Revenues that offset the above costs include credits gained from discharge and tipping fees for the waste feedstock and potential revenue from selling byproducts (*e.g.*, CO_2, biochemicals, *etc.*). The carbon intensity (CI) per kilogram of H_2 produced from corn stover is summarized in Fig. 7b, reaching a net removal of CO_2 when carbon capture and sequestration are employed. The TEA model is based on the process flow diagram shown in SI Fig. S2.

3.1.3. Target metrics for the integrated DF-MEC system. A key advantage of the DF-MEC system over abiotic H_2 production is the ability to recover H_2 from complex and polymeric substrates such as cellulose and hemicellulose that are abundant in many mixed waste streams. The success of the $BioH_2$ route hinges on its competitiveness with other H_2 technologies with similar or lower CI.[108] Key metrics contributing to the cost of $BioH_2$ are summarized in Fig. 8. Various permutations of these parameters bound by practical limitation remains a subject of exploration (Table 3). $BioH_2$ production approaches near-term target of \$2 kg^{-1} with economies of scale that lower the capital cost (*e.g.*, electrodes and membrane), high current density generation at the anode (improves the $BioH_2$ yield), and lower electricity cost. Selection of waste feedstock that allows revenue generation from discharge and tipping fees (*e.g.*, solid food waste and wastewater from cheese whey production process that is high in chemical oxygen demand) (Fig. 8) is critical to lowering the $LCOH_2$ for $BioH_2$.

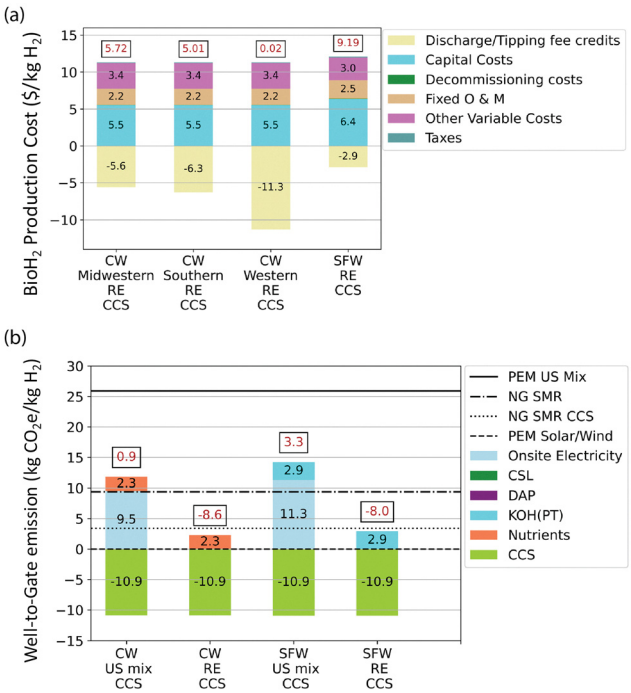

Fig. 7 Summary of biohydrogen production cost derived from TEA analysis (a) and well-to-gate CO_2 emission (b) per kg of H_2 generated. Wastewater from cheesy whey production and solid food waste were used as the feedstock for the case study. Renewable electricity derived from wind and solar was used. The analysis demonstrated the proof-of-principle that savings from tipping fee and discharge fee which varies substantially across midwestern, southern, and western regions lowers the production cost. Well-to-gate CO_2 emission varies by the source of electricity, grid (US mix) *versus* renewable electricity. Carbon capture & sequestration (CCS) can further bring the net CI to negative (removal of CO_2) in the scenarios when RE is applied.

3.2. What successful biohydrogen brings

In principle, $BioH_2$ has a decarbonizing potential unmatched by any other water-splitting technologies (Fig. 7). When CO_2 and H_2 gases are co-released from a biorefinery, it is carbon neutral as the co-produced CO_2 originates from the atmosphere. Carbon-negative $BioH_2$ is achieved when the relatively concentrated source of CO_2 co-produced with $BioH_2$ is removed through point-source carbon capture and sequestration (CCS).[108] It thus offers a means to decarbonize heavy industry, transportation, and places where reducing emissions has been challenging. By harnessing the energy generated from the degradation of organic feedstocks *via* living organisms, electricity use for $BioH_2$ production *via* integrated DF-MEC (23.9 kWh kg^{-1} H_2) could require less than half of the electricity typically needed for PEM water electrolysis (55.5 kWh kg^{-1} H_2).[120] In addition, the $BioH_2$ process permits degradation of solid lignocellulosic biomass with lower energy intensity than H_2 produced from gasification/pyrolysis which tackles solid organic wastes with temperatures ranging between ~250–1150 °C. $BioH_2$ also provides an opportunity to monetize domestic wastes, diversify H_2 sources, and increase energy access to rural and farming communities, similar to the PEC pathway.

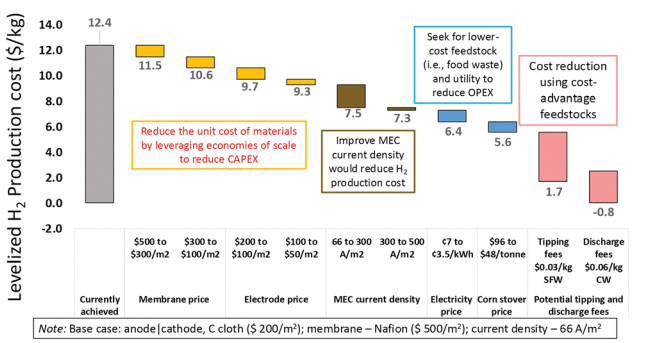

Fig. 8 Levelized H_2 production cost gets progressively lower as the capital cost is lowered, MEC current density increases, electricity and feedstock cost decreases. Tipping fees or discharge fees associated with low value waste streams bring revenue to further reduce the levelized production cost.

Table 3 Summary of cost drivers and target

Parameter	Units	State of the art	Ultimate target
Feedstock cost	\$ tonne^{-1}	\$86.68 for herbaceous biomass[117]	Low-cost, Negligible, or permits revenue from discharge or tipping fees
Bioreactor feedstock loading for fermentation	kg feedstock per L reactor volume	Trade-offs between feedstock deconstruction/utilization and feedstock loading beyond $\sim$ 25 g L^{-1} as cellulose	$\sim$50–100 g L^{-1} loading with $\geq$80% conversion
Yield (molar, per feedstock)	mol H_2 per mol sugar, [a]kg H_2 kg^{-1} biomass	<1 to 3.2 (trade-offs observed between sugar/feedstock loading and yield)	$\geq$3.2[107]
H_2 productivity	L H_2 per L reactor volume	Fermentation: 6.6 (batch operation) and 24.8 (fed-batch operation) both using deacetylated and mechanically refined corn stover MEC: 81 $\pm$ 3 L H_2 L^{-1} day^{-1} (synthetic)[118] 22.2 $\pm$ 6.2 L L^{-1} day^{-1} (real waste stream)[119]	TBD. Best to what experiments can achieve. Remained to be assessed with different feed stream and as a function of the reactor design/architecture.
Current Density	A m^{-2}	5–66[b] (unpublished data from fermentation wastewater generated from DMR);[118] 50 using synthetic media as MEC feedstock[118]	1000[d]
Electrode Cost	\$ m^{-2}	\$200 m^{-2}	\$20 m^{-2}
Electricity Cost	\$ kwh^{-1}	\$0.07 kWh^{-1}	\$0.01 kWh^{-1}
Cost	\$ kg^{-1} H_2	12.4[c] (with assumptions)	2

[a] Note: high molar yield leads to high H_2 production per unit of feedstock. [b] Highest H_2 productivity and current density were achieved from separate settings. [c] \$12.4 per kg H2 assumes 80% conversion of the feedstock biomass to hydrogen. [d] Ultimate target for MEC current density is purely based on a TEA model of an integrated DF_MEC system and the data is not published yet.

3.3. Targets, barriers, opportunities

3.3.1. Targets. As summarized in Table 3, meeting a BioH_2 production cost of \$2 per kg H_2 or lower requires advancements to be made in utilizing low-cost feedstocks, increasing yield and productivity, which necessitates processing and rapidly converting high loadings of feedstock to H_2 in dark fermentation and increased current density in MEC, while reducing the cost of the MEC electrode.

3.3.2. Barriers. Amongst several technical components that comprise dark fermentation and MEC, top challenges impacting technoeconomic feasibility lie in feedstock, conversion processes, process integration and scale-up. Research opportunities pertaining to feedstock lie in its sourcing, deconstruction, utilization, and characterization. The microbial feedstock conversion efficiency and H_2 yields as well as reactor designs and bioprocess conditions remain to be improved. Unit operations need to achieve compatibility during process integration and scale up while maintaining the target throughput. Success also hinges on durable, low-cost materials and robust operation at scale.

3.3.3. Opportunities

3.3.3.1. Fermentative H_2 production. Dark fermentation for H_2 production is an anaerobic process where microbes break down organic feedstocks into H_2, CO_2, alcohols, and volatile fatty acids.[121] Organic materials including agricultural and food wastes and wastewater are typical feedstocks for DF due to their cost-competitiveness and the environmental concerns around cleanup of waste materials. Microbial communities indigenous to the feedstock or obtained from other sources (*e.g.*, anaerobic digester granules) featuring broad metabolic diversity have been utilized in DF processes.[121,122] Alternatively, defined single and mixed-culture species have been explored for H_2 production,[114,122,123] which prevents metabolic competitors from dominating the populations and eliminates H_2 consuming bacteria like methanogens. Common bacteria found in DF includes those from the genera of *Acetovibrio*, *Caldicellulosirupter*, *Clostridium*, and *Thermoanerorobacterium*. These bacteria contain specialized, lignocellulolytic enzymes to breakdown recalcitrant and complex polysaccharides found in waste streams. These microbes' innate ability to produce these enzymes allows them to deconstruct biomass, consume sugars, and produce H_2 in one step, which has been termed consolidated bioprocessing (CBP).[124] Despite various efforts to optimize combinations of feedstocks and microbes, the optimal route to achieve economically viable BioH_2 production *via* DF is yet to be explored.

Achieving efficient conversion – the maximum yield of H_2 from the complete oxidation of biomass-derived sugar is 12 mol H_2 mol^{-1} hexose (C6, glucose, *etc.*) and 10 mol H_2 mol^{-1} pentose (C5, xylose, arabinose, *etc.*). However, the theoretical limit for DF is 4 mol H_2 mol^{-1} hexose and 3.2 mol H_2 mol^{-1} pentose,[107,125] as the microbes co-produce partially oxidized organic carbon products that do not allow complete recovery of the electrons contained in the feedstock as H_2. With each substrate containing different amounts of sugars, maximum yield on various biomass substrates ranges from 11 to 21 kg H_2 kg^{-1} substrate based on models by Solowski *et al.*,[126] highlighting the impact of feedstock selection.

Achieving high H_2 molar yield (per mol of sugar embedded in the biomass) hence leads to high H_2 yield per unit of starting feedstock. However, the trade-off between feedstock/sugar loading and H_2 molar yield underlines the importance of metabolically moving electrons efficiently to the H_2 synthesis pathway in the cells at high loadings of biomass. The capacity to process high loads of feedstock also reduces the demand for a large bioreactor footprint, an important cost driver. However, overflow metabolism characterized by production of an array of amino acids and alcohols was observed in the model cellulose-degrading

bacterium *Clostridium thermocellum* when high substrate loading (100 g L^{-1} avicel also known as crystalline cellulose) leads to an increased rate of substrate utilization.[127] Eliminating loss of electrons through side reactions remains critical in achieving high H_2 yield. For instance, eliminating lactate[128] and ethanol[129] production have shown to increase H_2 production and remains a vital approach.

Biomass deconstruction to fully unlock the available sugars within the feedstock requires additional testing of recombinantly expressed enzymes to break bonds linking various types of sugars for microbial utilization. CBP operation at high solid ratio typically result in incomplete fermentation by the candidate organisms as they stop breaking down the biomass and growth despite having food (*e.g.*, lignocellulosic substrate) at their disposal.[130–136] This decreases titers, rates, and yields, which adds cost to production. It is therefore critical to understand the underlying metabolic regulations governing sugar utilization as well as mechanisms inhibitory to both lignocellulose deconstruction and microbial growth.[131,132,134,137] To-date, inhibition has been attributed to multiple metabolites such as (1) short to medium chain acids; (2) lignin derived compounds produced during fermentation that disrupt the membrane proton gradient and integrity;[138–140] (3) HMF (hydroxymethylfurfural), furfural, and phenols that damage DNA, proteins, and membrane;[141–143] and (4) deconstruction intermediates like sugar-oligomers.[132,134] Molecules secreted such as quorum signalling peptides (*e.g.*, AgrD-type cyclic peptides) and metabolic products such as organic acids made by the microorganisms may also signal the cells to stop growth.[144] Eliminating the production of such signal peptides may be possible by disruption of the secretary mechanisms or pathway through targeted gene deletion. Process engineering such as separation or dilution of the fermentation broth remained to be explored. Identifying specific metabolic inhibitor(s) and mechanisms as well as strain modification/engineering and feedstock pre-treatment to overcome growth inhibition and hurdles in feedstock utilization is urgently needed.

Redox cofactors (NAD(P)H, ferredoxin) are known to mediate electrons obtained from sugars to hydrogenases for H_2 production. In *C. thermocellum*, both NiFe- and FeFe-types of hydrogenase are present based on genome information[145] yet their role in H_2 production/oxidation and their associated redox cofactors (*e.g.*, NADH *vs.* NADPH) are unknown. Such basic understanding will inform a genetic engineering strategy to maximize electron flux toward H_2, as biochemical reactions which divert the electrons away from H_2 production to side reactions or metabolites can be potentially inactivated by targeted gene deletion.

Feedstock supplies, selection, and processing – lignocellulosic biomass is one of the most abundant sources of carbohydrates suitable for CBP. The Billion Ton Report[146] identified up to 1.5 billion tons of total biomass resources in the form of dedicated energy crops, agricultural residues, logging residues, municipal solids, waste resources including animal manure and wastewater sludge, algae, and industrial CO_2.[146] Premiums paid to address and remediate a waste stream (*e.g.*, tipping fee) bring revenue to offset BioH_2 production cost. Locally sourced biomass, such as industrial food waste streams, requiring minimal processing and transportation will reduce cost and meet near-term needs for DF. However, as the industry scales up, more sophisticated logistics supply chain operations will be required to aggregate, store, preprocess, and formulate material. Depot models utilizing blending and formulation have been proposed to economically deliver an on-spec commodity product,[117,147] similar to that of the oil and gas industry that utilizes midstream operations to manage variability upstream and deliver on-spec products downstream.

While lignocellulosic biomass is primarily composed of cellulose, hemicellulose, lignin, and ash, the ratios of these components can vary depending on different biomass types, anatomical fractions, and tissue types, which all introduce variability challenges in downstream processing operations.[148] For example, the rind and vascular bundles of corn stover are rich in lignin, creating rigidity for the plant but also contributing to its recalcitrance to decomposition in comparison with the carbohydrate-rich pith tissues.[149] Targeted pretreatments and extractions can improve DF performance. For example, hot water treatments target hemicellulose removal to prevent the buildup of xylo-oligomers that can be fermentation inhibitors in DF, meanwhile providing recalcitrance reduction in the lignocellulosic matrix such that carbohydrates are more readily available.[117,147] Being effective in deconstructing the biomass, flexible to handle multiple feedstocks that are cost competitive, and robust in tolerating feedstock variability are key features of a viable technology.

Process integration and intensification – deployment of industrial-scale fermentative H_2 production necessitates maintenance of high volumetric H_2 productivity and high yields across long time scales, with minimal investment or downtime for cleaning and sterilization. Compared with bench-scale, low-intensity fermentations, larger-scale and higher-intensity fermentations are challenged by high viscosity mixing, higher partial pressures of dissolved H_2, and accumulation of soluble inhibitors generated as fermentation co-products or *via* feedstock solubilization. High production rates obligate high flux and throughput of biomass feedstocks, which is prone to reduce H_2 yields due to viscous rheology that impedes the uniform mixing required to maintain pH, dispersion of hydrolyzing enzymes, and an optimal dissolved gas concentrations.[150] Dissolved H_2 in the aqueous phase can adversely affect yields due to reaction equilibrium as H_2 is a product of a reversible reaction catalyzed by hydrogenase enzymes, which differs from the obligated H_2 production as a byproduct during nitrogen fixation by nitrogenase. Active removal of H_2 is therefore critical to maximize productivity, but these interventions must be applied while an optimal dissolved CO_2 level is maintained for microbial biomass production.[151] Moreover, H_2 removal by purging nitrogen gas imposes high costs for downstream gas separations; more scalable deployment strategies should therefore be targeted including thermophilic operation at high temperatures with low associated H_2 solubility, and improved mixing

geometries to maximize H_2 transfer to the headspace. Both mixing and gas removal configurations can be informed by computational fluid dynamics to reduce mixing times, eliminate unmixed dead zones in the bioreactor, and minimize required energy inputs.[152] Moving forward, computational models should be complemented with scale-down studies and biokinetic models to better inform the metabolic impact of heterogeneous conditions. Such studies would enable incorporation of biological dynamics into bioreactor computational fluid dynamics models, better informing the trade-offs between biological performance and the costs associated with maintenance of optimal, homogenous conditions.

To address soluble fermentation inhibitors, a combination of source reduction and reduced residence times for the inhibitor remains to be explored. However, balances need to be maintained between high flux of feedstock into the system, continuous removal of inhibitors in the aqueous phase, and retention of the bioconversion host. Continuous substrate addition has the additional benefit of continuous hydrolysis and liquefaction of solid feedstocks, reducing the characteristic viscosity of the system and improving mixing conditions. Use of continuous operational modes, including upflow anaerobic sludge blanket designs, has proven successful for long-term continuous operation with operational periods up to a year.[153] Despite the potential for contamination in long-term unsterilized cultures, biohydrogen production can be maintained over long time scales through a variety of strategies including selective enrichment of microbial communities,[154] or maintenance of thermophilic cultivations in pure cultures to reduce potential for outside contamination.[155]

3.3.3.2. Microbial electrolysis cell. MECs enable the transformation of biodegradable organic matter into H_2 gas *via* a combined microbial and electrochemical process. Exoelectrogenic microorganisms, which in MECs are localized at the anode, oxidize the dissolved organic matter through anaerobic respiration and transfer electrons to the electrode while releasing protons. The electrons are conducted through an external electrical circuit to the cathode where water is reduced, producing H_2 and hydroxide ions. By coupling organic matter oxidation with H_2 evolution, MECs can generate H_2 at a fraction of the thermodynamic voltage (0.14 V) required for abiotic water splitting (1.23 V) under standard conditions, while aiding in the removal of organic contaminants from used water. For industrial deployment, MECs need to be operated at commercial scale, enabling stable transformation of aqueous organic waste streams into H_2 gas at high rates and with high conversion efficiency. Achieving this goal requires upscaling of MECs from bench-top reactors (millilitres to Liters in volume) to commercial size systems (cubic meters in volume for individual units or larger) through electrochemical and bioprocess engineering.

Engineering MECs architecture for real-world applications – converting biomass into hydrogen using MECs requires reconciliation of electrochemical, chemical, and microbiological parameters that impact performance (Fig. 9). Small electrode spacing is needed to minimize the internal resistance of the cell and reduce the impact of low solution conductivity of typical waste streams on electrochemical performance. A small internal resistance in a compact MEC enables larger current and hydrogen production rates at a given applied voltage compared to less compact designs.[118,156–158] A small distance between the electrodes makes the use of separators often inevitable to avoid short circuiting of the cell (electrical contact between the electrodes) and to minimize hydrogen losses due to microbial consumption by hydrogenotrophs. Although several MEC studies favored the design of single chamber systems without separators, citing the high cost of membranes and their potential fouling, incorporation of separators remains the only practical approach for minimizing H_2 losses (*e.g.*, *via* methanogenesis) therefore increased energy efficiency.

Maintaining high current densities and stable operation in compact MECs will require careful management of solids and optimization of the solution chemistry. While waste stream pretreatment and new reactor designs can minimize solid accumulation, this aspect of MEC operation requires additional development. This issue is not relevant to any of the other

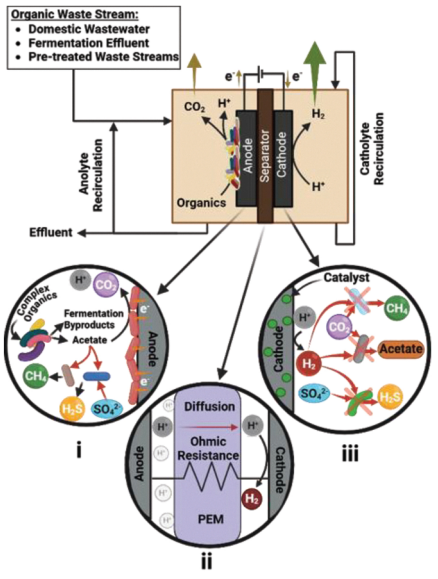

Legend:
Desired Microbes:
- Exoelectrogens (●) generate electric current.
- Fermenters and acetogens (●●●●) breakdown complex organics to simpler organics.

Undesired Microbes:
- Acetoclastic and hydrogenotrophic methanogens (● & ●) generate methane from acetate and hydrogen consumption, respectively.
- Homoacetogens (●) generate acetate from hydrogen consumption.
- Acetoclastic and hydrogenotrophic sulfate reducer (● & ●)
- Acetoclastic and hydrogenotrophic sulfate reducers (● & ●)

Fig. 9 Schematic of the most critical elements of a dual-chamber microbial electrolysis cell operating with DF effluent or real wastewaters. (i) Synergy between fermenters and exoelectrogens ensure current generation with complex substrates that cannot be immediately processed by electroactive bacteria. The presence of competing electron acceptors may reduce efficiency; (ii) reducing electrode spacing allows to minimize the internal resistance of the cell, overcoming the low conductivity of typical waste streams. (iii) Minimizing potential pathways for hydrogen consumption by methanogens is critical to maximize yield.

electrochemical technologies that reached commercial scale, as water electrolyzers and redox flow batteries operate with defined electrolytes with stable water chemistry.[159] Low buffer capacity (or alkalinity) of wastewaters is another challenge for maintaining stable and neutral pH across the cell.[160] MECs will need to be designed to cope with liquid streams that features wide variations in conductivity and pH. The use of separators with a high ionic conductivity such as anion exchange membranes can minimize the adverse impact of a low solution conductivity.[118,161] Effluents with high buffer capacities will deliver larger currents and produce more hydrogen by avoiding large pH gradients in the cell and a low pH near the anode, but this wastewater characteristics is not common. Continuous recirculation of a buffer-amended MEC effluent back to the fermenter or an upstream process can be a feasible approach to maximize performance *via* water chemistry optimization without any chemical losses in released effluents.

The long-term stability of MEC performance needs to be demonstrated *via* consistent current and H_2 generation over time. While the performance of bioanodes in small pilot systems is usually reported as steady, membranes and cathodes have shown rapid degradation due to biological and inorganic fouling. Thick biofilms, often featuring mineral precipitation, can develop within and on the cathode catalysts as well as on the membrane surface, restricting ion transport and increasing the internal resistance of the cell. Such performance degradation has been documented previously; however, no effective approaches for restoring performance without cathode replacement have been developed. Implementation of electrode cleaning is further complicated in systems with tightly spaced electrodes and usually requires complete disassembly of the whole stack. To enhance maintenance efficiency and reduce costs, novel techniques need to be developed for replacing cathodes or cleaning membranes, cathodes, and liquid chambers *in situ*. These methods should not necessitate disassembling the cell, nor should they disrupt the microbial community on the anode.

Engineering microbial communities for MECs – operation of MECs on aqueous waste streams that are highly variable in substrate composition using natural or engineered microbial communities offers different advantages. Due to their broad metabolic capacity, communities obtained directly from process wastewater, anaerobic digesters, or other waste treatment systems can improve substrate utilization, increase resilience to varying stream compositions, and lower inoculum and operational costs. MEC performance hinges on enriching specific microbial communities capable of maximizing the conversion of the various compounds in the feed stream into electrons. Typically, the indigenous communities consist of diverse species capable of metabolizing a wide range of organic substrates, from simple compounds like sugars and fatty acids to complex molecules like proteins and lignocellulose. Specialized microbes, such as fermentative bacteria, hydrolytic bacteria, and electroactive microbes, can work synergistically to degrade various substrates and transfer electrons to the anode. Robust and functionally diverse communities can dynamically shift their metabolic activity in response to changes in substrate composition, ensuring continuous operation even with fluctuating feed compositions. Over time, the microbial community evolves to enrich species best suited for the available substrates and MEC operating conditions. However, frequent variation in substrate composition can adversely affect anode performance, due to the lag time required by the community to adapt to the new feed source.

MEC operation can be optimized for substrate variability using several strategies. (1) Anode materials can be optimized to promote better microbial attachment and stability. As an example, carbon cloth electrodes allow microbial attachment and biofilm development.[156] In addition, 3D printing technologies with existing enriched microbial communities can be used to optimize MEC startup process.[156] (2) Pre-treatment of the feed stream can break down complex organic compounds into simpler substrates (*e.g.*, acetate), which are more readily metabolized by electroactive microbes.[162] (3) Process control by changing hydraulic retention time (HRT) can ensure microbial community has sufficient time to metabolize complex substrates. A shorter HRT is suitable for simpler substrates, while a longer HRT is better for complex or variable feeds. In addition, real-time process monitoring (*i.e.*, electrical current, pH) could inform adaptive feeding strategies. For instance, when current drops, the new substrates can be introduced gradually while allowing microbes to slowly adapt to new environments. (4) Enriching a wide range of bacteria which can break down carbohydrates, proteins, and lipids into more easily degradable volatile fatty acids or H_2 as well as convert/funnel other volatile fatty acids into acetate. Specifically enriching electroactive bacteria that can directly transfer electrons to the anode could improve electron transfer efficiency. (5) Operating MEC at favorable pH's and temperatures.

Scaling up MECs: the importance of minimizing internal resistance – Ultimately, MEC throughput should be increased when assembling industrial-scale reactors. Rigorous design specifications and approaches are needed to define how performance obtained at the bench scale can be translated into large-scale systems. Considerations should be given to both electrochemical and microbiological parameters as MEC dimensions are increased. Several studies have shown that the total electrode resistance normalized by area increases as the electrodes are scaled up.[163,164] Scale up studies should include the resistance of each electrode, and of the solution, to pinpoint the largest energy loss in the cell and drive future work toward its minimization. These resistances can be obtained by linearizing the slope of the total cell voltage and electrode potentials as a function of the current density. Previous scale up studies indicated that the internal area specific resistance (ASR) of a microbial fuel cell increased from 255 $m\Omega\ m^2$ at small scale (7 cm^2, 28 mL) with near equal electrode resistances (anode, 71 ± 3 $m\Omega\ m^2$; cathode, 66 ± 17 $m\Omega\ m^2$) and a higher solution resistance (118 $m\Omega\ m^2$) up to 880 $m\Omega\ m^2$ at large scale (4800 cm^2, 85 L) with a greater increase in the cathode (555 ± 24 $m\Omega\ m^2$) than the anode (238 ± 18 $m\Omega\ m^2$), and similar solution resistance (87 $m\Omega\ m^2$) (SI Table S1). Here, ASR is expressed in impedance $\times$ area because

it represents the electrical resistance multiplied by the charge transfer area, or equivalently, the voltage divided by the current density. These changes in ASR occurred despite the use of an identical reactor architecture, the same electrode materials, and the same wastewater source.[164,165] Such a large ASR (880 mΩ m^2) will translate into poor hydrogen production rates of 0.86 L H_2 $L_{reactor}^{-1}$ day^{-1} at 0.9 V (100 m^2 m^{-3} electrode packing density and onset voltage of 0.56 V), while current lab scale systems can produce >80 L H_2 $L_{reactor}^{-1}$ day^{-1} with an ASR of 8 mΩ m^2.[118] Reasons for these increased resistances during scale up must be elucidated and addressed to maximize hydrogen production rates. The challenges that arise by using very large electrodes could potentially be circumvented by scaling out. Meaning that rather than scaling up MECs, a large number of smaller reactors are connected together to increase overall throughput.[157]

4. Thermochemical hydrogen pathway

Similar to the other advanced pathways, TCH technologies have a rich history of ideation and development to evolve and demonstrate viable concepts over many decades. Detailed process chemistry and technology types have been demonstrated at various scales, and over multiple cycles, from laboratory to small pilot plant as described in comprehensive works dating from 2002.[166–171] Thematically, thermochemical water splitting cycles are defined by the number of reactions required to complete the cycle, and by the method of treatment (*e.g.*, purely thermochemical or hybridized approaches).[9,171–173] Examples of three common cycle chemistries are illustrated in Fig. 10.

The two-step non-volatile, non-stoichiometric redox-active metal oxide (MO_x) cycle is conceptually the simplest. The cycle chemistry is depicted in the far left panel of Fig. 10. In the first "reduction" step, a metal oxide like CeO_2 is heated to a high temperature where molecular oxygen spontaneously evolves from the crystal lattice under an appropriately low gas-phase oxygen chemical potential. At this moment thermal energy is directly converted into chemical potential energy. In the second "oxidation" step, the now oxygen-deficient $CeO_{2-\delta}$ is exposed to steam at a lower temperature where oxygen is stripped from the water molecule producing H_2. The second step is also spontaneous, and while the water-splitting process is surface mediated, bulk $CeO_{2-\delta}$ does not act catalytically. The defected oxide is "consumed" in the process to the extent allowed by bulk thermodynamics. The MO_x cycle is the subject of the present perspective because researchers in the TCH field have mostly abandoned alternative cycle chemistries given a myriad of technological challenges associated with the development of such alternatives.[171,174,175]

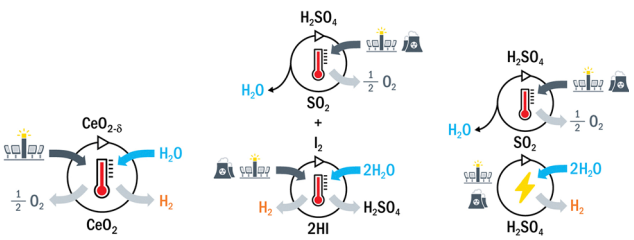

Fig. 10 Schematic showing exemplar thermochemical cycles. Far left is the simple two-step metal oxide cycle, center is the multistep cycle, and far right is the hybridized cycle that invokes an electrochemical step other than direct water electrolysis. Water and energy are the only inputs into these systems, and hydrogen and oxygen are the only outputs. Nuclear plants, solar and other sustainable power sources supply the energy inputs to these water splitting cycles. Adapted with permission from the Electrochemical Society, ref. 9, Copyright 2021.

Two general reactor configurations, batch or continuous, and two operational modalities, pressure/temperature-swing or pressure-swing only at constant (or near constant) temperature, respectively, have been employed to date.[176] The redox-active MO_x in these configurations function simultaneously in all cases as radiant absorbers and reactants that undergo thermochemical cycles governed by bulk material thermodynamics. In addition, materials within these reactors are either heated directly with concentrated solar radiation at flux levels of 100's to 1000's of suns into windowed receivers, or indirectly by irradiating the walls of opaque refractory containment vessels.[176,177] Large arrays of heliostats are proposed to concentrate the solar radiation and provide renewable heat at process temperatures in excess of 1500 °C, as well as provide power to the balance of system.[178] To date TCH H_2 production using redox-active MO_x cycles has been demonstrated at scales up to 750 kW_{solar}.

In this perspective, the current status of the TCH Hydrogen Pathway is examined to identify RD&D gaps, and to discuss the technical challenges that must be solved in order to realize commercial viability. In so doing, opportunities for the research community are outlined that address both fundamental science and engineering challenges crucial for achieving cost parity with other commercial or near-commercial H_2 production technologies in support of the H2@Scale initiative.

4.1. Current state of the art

4.1.1. Target metrics for TCH system. Commercial viability necessitates that TCH technologies establish metrics and specific performance targets that align with those of the DOE – like cost and efficiency – outlined in Section 1. These metrics allow for an objective comparison to other H_2 production technologies and thus reveal use cases where TCH is a competitive sustainable H_2 production pathway within the context of regionally specific H_2 demands. Equally important, TCH needs to demonstrate a credible path towards achieving these targets in order to engender stakeholder confidence, attract investment, and cultivate the collaborations necessary to further the RD&D needed to advance to higher TRL.

TCH metrics critical for evaluating process efficiency, viability, and scalability are listed in Table 4. These metrics not only reflect near-term operational capabilities, but also account for long-term upscaled performance and sustainability attributes. Values listed in Table 4 were derived through community consensus, with some examples taken from real-world demonstrations[179,180] or detailed system studies,[181,182] and

Table 4 Target metrics for a TCH process

Parameter	Units	Near term	Ultimate
STH efficiency	%	5.3[a]	25
Degradation (redox-active MO_x)	Δ% redox capacity per 10 000 hours	<20	<1
Lifetime (system)	years	5–10	30
Lifetime (redox-active MO_x)	% replacement per year	<50	<10
H_2O conversion	%	18[a]	>10
Max T_{RED}	°C	>1500[a]	<1350
Power density	kW_{fuel} m^{-3}	45[a]	>100
Material intensity	kg m^{-3}	5000[e]	1500
Material cost	\$ kg^{-1}	5.00	2.50
Energy utilization factor	kWh kg^{-1} H_2	166[b]	<100
System cost	\$ $kW_{H_2}^{-1}$	150–250[f]	<65
Cost (H_2)	\$ kg^{-1} H_2	4–7[cd]	<2

While there are multiple choices for converting between mass and energy for the H_2, 32.7 kWh kg^{-1} H_2 is used here. [a] Ref. 179 – based on HHV_{fuel} and reactor volume. [b] Ref. 183 – based on H_2 at STP. [c] Ref. 181. [d] Ref. 182. [e] Based on H_2 conversion system volume. [f] Based on $\Delta G^0_{l,H_2O}$.

encompass various dimensions such as lifetime and degradation rates, energy utilization and costs, while also considering the interplay between functional materials, reactor design, and overall system performance. For example, the energy utilization factor, set at less than 100 kWh kg^{-1} H_2 for the ultimate target, must be considered within the broader landscape of energy inputs and outputs determined by reactor design, operational modality, and anticipated future advancements in redox-active materials as well as improved separations and heat recuperation technologies.

Metrics such as system cost, currently targeted at less than \$65 $kW_{H_2}^{-1}$, should be benchmarked against established technologies to facilitate meaningful comparisons. Similarly, the redox-active MO_x degradation metric, which currently targets less than 1% reduction in redox capacity per 10 000 hours, must be evaluated against the operational lifetimes of existing electrolysis technologies, which can exceed 80 000 hours. Importantly, the establishment of a standardized energy utilization metric, suggested here as kWh kg^{-1} H_2, provides a common framework for comparing different H_2 production technologies that include other advanced pathways as well as conventional electrolysis. Using robust tools, standardized methodologies for TEA, and adherence to rigorous measurement protocols will ensure that these metrics are traceable across various RD&D efforts. Finally, ongoing research and technological advancements will inform the evolution of these metrics, necessitating a dynamic approach to their modification, refinement, and validation.

4.1.2. TCH benchmark system. An exemplar batch-type, windowed radiant cavity receiver is shown in Fig. 11.[180] It is widely considered the best performing design in terms of efficiency, power density, and gas conversion.[179] Incidentally, the European Union is host to the largest collection of upscaled TCH demonstration platforms featuring two-step non-volatile, non-stoichiometric MO_x water splitting cycles, including a plant supported by a 750 kW_{solar} power tower.[184–186]

With an exemplar reactor operating at 4 kW_{solar} input, Marxer *et al.*[180] demonstrated thermochemical gas splitting (CO_2 not H_2O) with 100% selectivity for carbon monoxide (CO) and O_2, achieved 63% peak molar conversion of gas feed,

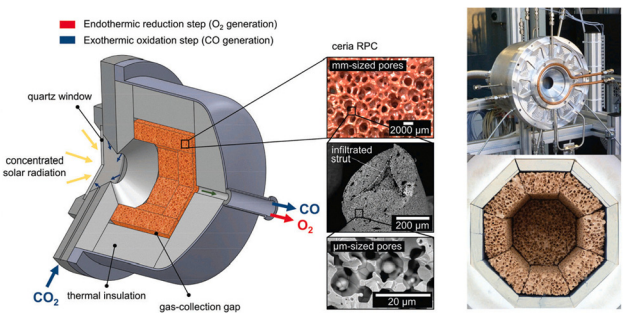

Fig. 11 A schematic and images of the directly-irradiated cavity reactor tested by ref. 180, reproduced with permission from the Royal Society of Chemistry.

and 5.25% solar-to-CO conversion efficiency (LHV basis) using pressure/temperature-swing operation. The demonstration was not halted by redox-active MO_x instability or hardware failure. In fact, this same design was upscaled to 50 kW_{solar} and deployed on a tower at IMDEA Energy in Spain under the EU Horizon 2020 Sun-to-Liquid Project[187] where CO_2 and H_2O were co-split producing ~5200 L of synthesis gas (a mixture of H_2 and CO) over 62 thermochemical cycles in a dedicated campaign lasting nine days.[188] Significantly, the authors report a 4.1% solar-to-syngas conversion efficiency (similar to STH) at this scale without implementing heat recuperation, and further speculate greater than 20% conversion efficiency is achievable by recovering rejected heat. The impact of design and system variables were later explored by Zoller *et al.*,[189] where the authors developed and validated a heat transfer model at the 50 kW scale, and determined that >10% energy conversion efficiency was achievable even without heat recovery. A follow-up project called Sun-to-Liquid II was launched in 2023 and aims to demonstrate a reactor efficiency of 15%.[190]

Cerium oxide ($CeO_{2-\delta}$) is considered the state-of-the-art material,[176,191–193] and not surprisingly was incorporated into the most recent exemplar reactor demonstrations. Its use in a two-step cycle was proposed in 2006,[194] and demonstrated in a solar reactor in 2010.[195] Ceria offers key advantages for the TCH process: fast redox kinetics,[191] long-term thermal stability[195]

and unique thermodynamic properties[196,197] that enable it to split water at relatively high temperatures and with a small temperature swing of 200 °C.[196] Notably, ceria is the only non-stoichiometric MO_x material known to maintain favourable water splitting thermodynamics at conditions of extremely low gas-phase oxygen chemical potential encountered when substantial amounts of H_2 and water vapor coexist in the oxidizing environment. This is due to ceria's unique electronic structure and O-defect formation mechanism that manifests a large entropy of reduction.[198–201]

4.2. What does success look like for TCH technology?

Similar to the other advanced pathways, success is predicated on continued technology advances and demonstration at large scale, while meeting critical performance targets. The technology must demonstrate high energy efficiency (or low energy utilization), scalable systems with high reliability, and reduced costs for components like reactors, heat exchangers, separation units and heliostats that are capable of producing H_2 with minimal reliance on grid electricity. Some consider integration with thermal energy storage important for enabling continuous operation and improving economic viability, as high annualized capacity factors can significantly reduce $LCOH_2$ particularly for capital-intensive technologies aiming to achieve cost parity with current H_2 market prices.[202] Furthermore, in a resource-limited funding environment, pragmatic decisions about demonstration projects focused on low-risk, high-reward gains are essential. Achieving TCH commercial viability will require successfully demonstrating system integration at scale, notwithstanding the inevitable ongoing pursuit of novel designs and materials at smaller scale to push the physical limits of energy conversion efficiency. Integrated systems include storage for flexible H_2 output, innovative reactor designs that permit efficient solid–solid heat recovery, and deployment models that allow for co-location with solar towers *or* advanced nuclear reactors with long-term operational stability even if these early demonstration systems do not achieve optimal design-point efficiencies.

4.2.1. Scalable reactor designs. Scaling up the two-step redox-active MO_x TCH pathway to relevant sizes, such as modular systems greater than 50 kW and full systems exceeding 1 MW, is a challenging endeavour but essential for proving commercial viability. Importantly, gathering system and operational cost information, as well as documenting real-world experience at these scales, is necessary for rigorously evaluating economic competitiveness so that industry can make informed partnership and investment decisions.

At the moment, the choices of TCH reactor type (batch or continuous), operational modality (pressure/temperature swing or pressure-swing only, direct or indirect heating), and the redox active material combine to offer many potential candidate designs and operating modes for upscaling, each with its own key performance parameters, initial TRL, and challenges.[176] A directly-heated batch-type reactor operates in discrete cycles where a redox-active MO_x is heated, reduced, cooled and then re-oxidized in separate phases within the same cavity. The functional material is fixed inside this cavity and exposed to pressure/temperature-swing cycling, which results in non-continuous H_2 production (see Fig. 11); O_2 separation is achieved temporally. The *basic* continuous-flow direct-heated reactor is comprised of two cavities, one held at the higher reduction temperature and the other at the lower re-oxidizing temperature with MO_x transported between the two cavities. H_2 and O_2 are produced continuously and O_2 separation is achieved spatially. In either configuration, pressure swing is managed by application of vacuum or inert gas sweep to generate the low O_2 partial pressure required for MO_x reduction.

The main differences between batch- and continuous-types are: (1) system complexity, (2) active material inventory and management, and (3) heat recovery – all of which affect system cost and design-point efficiency leading to trade-offs when considering scalability. For example, the batch-type reactor is simpler to design and possibly less costly to build and operate than a continuous-type, but encounters significant challenges when scaling to MW levels due to the large quantities of redox-active material required and the complexities of maintaining uniform absorptance of concentrated solar irradiation in large receivers. Additionally, since the material is fixed inside one cavity, practical limitations restricts heat recovery to gas-gas and gas-solid precluding direct solid–solid. In other words, effectively recuperating heat from the solid when cycling between the reduction and re-oxidation temperatures, or even recovering the re-oxidation exotherm for that matter, is prohibitively difficult in fixed-bed devices.[203,204] Indirect heating of the redox-active solid, while appealing because it eliminates engineering challenges associated with windowed receivers, increases heat transfer resistance requiring the directly irradiated containment vessel to operate at much higher temperatures than a like-type windowed receiver. Due in part to these design challenges, the highest achievable STH efficiency of the batch-type system is fundamentally limited and predicted to be lower than a continuously operating reactor.

Continuous-type reactor designs are more complex due to the challenges of conveying MO_x material in harsh thermal and mechanical environments that need to maintain a hermetic seal (*i.e.*, gas separation) between the two cavities and the ambient environment. However, the ability to operate continuously delivers stable H_2 production rates and improved thermodynamic performance engendered by designs that utilize counter-current flow between the reacting solids and gases to maintain more favorable chemical potential gradients within reduction and re-oxidation zones.[205,206] Additionally, continuous-type reactors offer a direct means to recuperate heat from solid reactants and require much less redox-active material to operate because the oxide is not stored inside the cavity receiver. And while these design features may ultimately greatly increase STH and overall system efficiency relative to batch-type, very few continuous-type concepts have been tested,[207,208] and none have yet achieved better performance than the exemplar batch-type design.

4.2.2. Considerations for deployment at scale. Beyond choices made for a particular reactor design and operating mode, successful TCH deployment at scale is driven primarily

by overall system efficiency and material reliability. Here, the system includes solar field and balance of plant components to support the reactor such as piping, pumps, separations units, heat exchangers, steam generators, *etc.*, that are fully integrated into a chemical plant producing 100 tonnes H_2 day^{-1}.[181] Balancing these factors is not trivial. Low TRL prototypes have prioritized pushing to higher temperatures and higher fluxes by using directly irradiated receiver-reactor systems in order to maximize metrics like chemical conversion and fuel yield because TCH will need to reach greater than 20% annual efficiency and operate at a much higher power density to become competitive with electrolysis.[179,209] This approach creates significant challenges related to the durability of materials exposed to thermally harsh conditions of high radiant flux and large temperature gradients. The need for high concentration ratios to limit re-radiation losses also brings with it the challenge and costs associated with a solar field designed to achieve them. Furthermore, in the past decade it has become clear that for any solar thermal technology to be economically competitive with a solar electric technology, heat recuperation and potentially thermal energy storage must be integrated into a TCH chemical plant.

An alternative pathway to that of directly irradiated receiver-reactor concepts (windowed or indirect) is also under development seeking to avoid the large re-radiative losses at the primary aperture and material failure due to strong thermal gradients. This approach is indirect in which the solar heat collection is *decoupled* from the chemical reaction using a heat transfer fluid. In 2019, a novel solar receiver was developed that achieves fluid temperatures of 1550 °C at a receiver efficiency exceeding 80% with a relatively moderate concentration ratio of 1000 suns. This high temperature, high efficiency receiver accomplishment exploits the ''greenhouse'' effect of polyatomic gases to reduce re-radiative aperture losses.[210] Using a fluid to indirectly heat redox-active materials that are confined in fixed or moving beds does add heat transfer resistance but avoids direct exposure of functional materials to high-flux irradiation that accelerates thermal degradation. More importantly, heat recuperation and storage, which enhance overall system efficiency, is significantly easier because the heat transfer fluid circulates throughout the process but does not contact redox-active material. Such TCH schemes operate at a lower temperature (to lessen the material stability challenge) and with lower energy conversion efficiency, but fundamentally incorporate heat recuperation and storage. In addition, other benefits to decoupling solar collection from chemical reactions include the ability to better design each receiver and reactor component separately and, in the case of a packed-bed thermochemical reactor, adopt designs more commonly used in the chemical industry.

4.3. Targets, barriers, and opportunities

4.3.1. Targets. Target metrics for a full TCH system presented in Table 4 align with overcoming the barriers to technology development introduced in Section 1. While these metrics address the systems-level, a full complement of redox-active material performance targets are also important to assess the commercial viability of a two-step redox-active MO_x cycle. Community consensus specific to these materials is beginning to emerge from DOE's HydroGEN Advanced Water Splitting Materials Consortium[211,212] and is briefly summarized in Table 5.

The material efficiency target, which is a different standard than STH, is derived from the free energy needed to split water normalized by the reaction enthalpy of MO_x reduction. This value is the maximum theoretical efficiency a MO_x material can attain in a two-step water splitting process[213] and reveals the importance of discovering water-splitting oxides that have a lower reduction enthalpy than CeO_2; such materials would cycle at lower temperatures and are inherently more thermodynamically efficient thus positively impacting systems-level performance markers as discussed earlier. Aside from kinetic performance, the remaining parameters are metrics that relate fundamentally to the magnitude of a MO_x's reduction entropy and will be discussed shortly. Here, materials are characterized by measuring H_2 production capacity in an oxidation environment that co-mingles steam and H_2; representative of a ''high [steam] conversion condition''.[214]

Taken together, the targets expressed in Tables 4 and 5 stimulate innovation in material discovery and in the design of complex thermochemical systems necessary to overcome current barriers to advancing the TRL of TCH technologies. Among recent RD&D efforts exploring new non-stoichiometric MO_x materials are a set of focused, long-term projects coordinated through DOE's HydroGEN Advanced Water Splitting Materials

Table 5 Target metrics for TCH redox materials

Parameter[b]	Units[a]	Descriptor	Ultimate
Material efficiency	%	Thermal efficiency of two-step process $\left(\frac{\Delta G^0_{WS}}{\Delta H^0_{RED}}\right)$	>50
Reduction capacity	—	mmol O mol^{-1} atom in solid	5×
H_2 production capacity (100% steam)	—	mmol H_2 mol^{-1} atom in solid	5×
H_2 production capacity (oxid. @H_2/H_2O of 0.001)	—	mmol H_2 mol^{-1} atom in solid	2.5×
H_2 production capacity (oxid. @H_2/H_2O of 0.01)	—	mmol H_2 mol^{-1} atom in solid	1×
Kinetic performance	—	Time to 90% of H_2 produced at max yield	0.20

[a] Unitless targets normalized to values measured for CeO_2 cycled at ΔT = 550 °C and 10 pa O_2. [b] Measured at specific redox cycle conditions (see ref. 212).

Consortium, which is a highly collaborative initiative launched in 2017.[215]

4.3.2. Barriers. Realizing performance targets in TCH systems is challenged by knowledge gaps in our understanding of both materials (redox active as well as containment/support) and the integration of complex subsystems operating in extreme thermal and mechanical environments. Several areas where focused RD&D should be prioritized to advance the TRL necessary to achieve commercial-ready status are: (1) active materials, (2) reactor and auxiliary system design, (3) system integration, and (4) TEA and life cycle analysis (LCA); all of which are important to realizing TCH production plants with long-term operational stability, scalability, and competitive costs. Regarding materials, current redox-active MO_x's such as ceria and perovskite oxides have limited H_2 production capacity per cycle and are susceptible to thermal degradation. The few reactors that have been used for demonstrating two-step water splitting chemistry with non-stoichiometric MO_x are inefficient, relatively small-scaled research instruments lacking industrialized features. Their small scale also results in economic uncertainty that limits stakeholder confidence and investment readiness due to a lack of standardized, robust TEA methodologies and benchmarks for analyzing real-world deployment scenarios.

To overcome these barriers, RD&D opportunities exist in the discovery of materials with superior reduction behavior at less extreme conditions that exhibit fast kinetics, highly stable cyclability, and high water conversion extent at practical re-oxidation temperatures. There is also opportunity for engineering material form factors to better utilize solar absorptance, together with improved heat and mass transport. Innovative, robust, minimal maintenance reactor concepts are needed that can efficiently scale to >1 MW and be compact enough to facilitate modularity or simplicity in installation while achieving a high power density. Auxiliary systems with advanced heat exchange and separations that take full advantage of thermal energy storage and system integration are essential to meet the energy utilization target and achieve ultimate scalability. Finally, robust methods for conducting detailed TEA and LCA[216] informed by engineering data collected from upscaled systems, which account for transient operation, are needed to improve our understanding of – and build upon our knowledge of – key relationships that can be leveraged to reduce costs and explore optimal trade-off strategies.

4.3.3. Opportunities. The maturation of TCH technology presents the research community with opportunities to tackle both fundamental science and engineering challenges crucial for achieving H2@scale objectives. These challenges encompass addressing performance issues outlined in Section 1 by continued investment in traditional ideas that implement derivative knowledge, as well as exploring innovation through the pursuit of novel processes or system integration strategies that extend TCH beyond the purely thermochemical realm, as well as beyond simple water splitting chemistry. Notably, TCH can directly utilize CO_2 in co-splitting cycles, creating a valorization pathway for carbon capture and utilization. This advantage is especially attractive for co-location with industrial emitters or biogenic CO_2 sources, turning emissions into high-valued chemical feedstocks.

While it is important to recognize the value of investing in demonstration projects focused on low-risk and high-reward gains (*i.e.*, application of derivative knowledge), it is equally important to recognize the potential of data science and machine learning to enhance material discovery, as well as explore how cycle hybridization or chemical looping integration can enhance overall process efficiency.

Computational material science – RD&D opportunities exist to help close knowledge gaps and increase our understanding of TCH material redox behavior. Efficient water splitting materials require not only favorable thermodynamic properties, determined by the energetics and defect formation mechanism of a lattice oxygen vacancy, but also optimized kinetics manifested through careful tuning of defect chemistry and structural stability.[217,218] In addition, an efficient water splitting material must be durable enough to remain stable over many thousands of redox cycles at high temperature, and at extremely low gas-phase oxygen chemical potential, which thermally and chemically stress the crystal lattice on every cycle. Stability and durability of the MO_x are a direct result of degradation mechanisms underpinned by fundamental physical and chemical driving forces that result in phase evolution, phase separation, dissolution, sintering, and reactions at interfaces. Given the clear need to discover better performing materials, opportunities to conduct both derivative and fundamental research abound.

Since the emergence of ceria as the preferred non-stoichiometric MO_x in two step cycles – supplanting iron oxides – there has been a concerted effort to modify its thermochemical behavior while preserving the fluorite structure and its unique redox properties.[193,219] Substituting percent levels of Sm, Hf, or Zr for Ce proved useful in reducing the reduction enthalpy and lowering the reduction temperature, however, reduction entropy also decreased which lessened the thermodynamic driving force for water splitting.[220] Similarly, a promising group of Mn-based perovskite oxides emerged – $La_{1-x}Sr_xMn_{1-y}Al_yO_3$[221] and $BaCe_{0.25}Mn_{0.75}O_3$[214] – that reduced to a much greater extent than ceria at temperatures $\sim$1350 °C; however, these oxides also suffered from low reduction entropy relative to CeO_2. Therefore, as the field continues to pursue derivative studies on small classes of materials, there is a clear knowledge gap in our understanding of how to modify and/or formulate the MO_x composition and electronic structure needed to increase reduction extent at lower temperature while simultaneously preserving high water-splitting efficacy.

Stepping into this gap is a new and exciting era of TCH materials-by-design using first-principles theory and machine learning. Computational frameworks have systematically demonstrated their ability to identify and evaluate promising candidates. Beginning with Wolverton and colleagues, who pioneered computational approaches to screen oxygen vacancy energetics, phase stability, and cation redox potentials in novel

perovskite oxides,[201,222,223] others followed using physically intuitive models[218] or crystal graph neural networks trained by density functional theory (DFT)[224,225] to capture complex relationships in crystal structures needed to predict and screen for redox activity. These works not only highlight the interplay between local bonding environments and defect formation energy, but have resulted in a substantial increase in the number of compounds predicted to split water under TCH reactor conditions.

One notable outcome of these frameworks is the discovery of $Ca_{2/3}Ce_{1/3}Ti_{1/3}Mn_{2/3}O_3$ (CCTM2112).[226] Briefly, first-principles calculations identified CCTM as a stable perovskite oxide with favorable redox properties through the following steps – the oxygen vacancy formation energy was predicted to be 3.30 eV placing it within the optimal range for redox cycling and lower than that of CeO_2, convex hull analysis confirmed phase stability under water splitting redox conditions, and electronic structure analysis revealed both A-site $Ce^{4+/3+}$ and B-site $Mn^{3+/2+}$ redox activity that is a very novel finding for a perovskite oxide. Predictions were validated experimentally. This example highlights the transformative role of computational methods—first-principles calculations and machine learning—in identifying high-performance redox-active materials. Other groups funded by DOE's HydroGEN[215] consortium have also demonstrated equally successful computational frameworks tailored for TCH material discovery by enabling targeted predictions of thermodynamic and structural properties. Ample opportunities remain to continue improving the predictive power of these frameworks by extending models and workflows. For example, more training data and experimental validation are needed to capture MO_x features of solid solutions, and to improve model accuracy for ''unseen'' crystal structures.

Engineered material shapes of form factors – recently, researchers have accepted the thermochemical limitations of CeO_2 and instead focused on improving STH efficiency by enhancing the capture and utilization of solar energy within the material. This is accomplished by modifying the geometric shape of ceria inside the solar reactor. Casting ceria into reticulated porous ceramic structures revealed that high surface-area engineered forms greatly increases gas–solid contact enhancing heat transfer rates and reaction kinetics.[227,228] Building on these observations, other works cast ceria into various shapes *via* 3D-printing and found such ordered structures performed better than reticulated porous ceramic, especially at controlling temperature gradients through large sections of material.[229] The 3D-printed materials not only achieved a higher and more uniform temperature profile compared to that of state-of-the-art reticulated structures, but increased the specific fuel yield per unit volume for the same solar radiative flux input, which directly improves both power density and energy utilization. Engineered structuring of redox-active MO_x is at the forefront of modern TCH reactor design and opportunities continue to evolve where baseline structures can even be chemically modified to enable or enhance performance, essentially activating inert support material to potentially lower costs.[230]

Alternative redox strategies – the high temperatures required to reduce a non-stoichiometric MO_x can be decreased without manipulating the crystal's electronic structure, as is currently practiced, if chemical reducing agents such as methane are introduced into the reduction step. While this is common practice in the carbothermal reduction of oxide ores in the metallurgical industry using solid forms of carbon, and has been proposed and demonstrated specifically for solar syngas production with fully-stoichiometric redox cycles,[169] this alternative is much less commonly proposed for non-stoichiometric oxide cycles and thus presents an opportunity to explore benefits and design trade-offs for TCH.

Taking CeO_2 as the example, a small number of experimental[231,232] and theoretical[233] treatises have been published that show much higher reduction extents for CeO_2 (defect concentration – $\delta > 0.2$) can be obtained at temperatures less than 1000 °C. Major advantages to this alternative processes are: (1) a lower reduction temperature enables easier coupling to thermal heat sources and reduces re-radiation losses to the environment, and (2) the need for heat recovery is greatly reduced, or in the case of ceria heat recovery is completely eliminated. In fact, Krenzke and Davidson[233] predict a solar-to-fuel conversion efficiency of 39% for CO_2 splitting and 40% for H_2O splitting without heat recovery using methane-driven reduction. Syngas formed during MO_x reduction can be converted predominantly to H_2 using conventional water-gas shift technology, though equilibrium constraints typically leave traces of CO or CH_4[234] which may require gas cleanup depending on H_2 purity requirements. Regardless, high-purity H_2 can be obtained in the re-oxidation step when feeding only steam.

Short of producing pure H_2 using carbothermal reduction, syngas itself is a flexible intermediate for synthetic fuels, chemicals, and materials. Thus an opportunity exists to position TCH as a bridge to carbon-based circularity even if H_2 generation becomes a lesser priority. Importantly, coupling carbon capture and sequestration to the process, or using biogas instead of natural gas as the reductant, would drastically reduce the industrial emissions from conventional H_2 production *via* steam methane reforming.[235]

Another underexplored pathway towards alternative reactor concepts aimed at reducing the reduction temperatures of the redox-active MO_x is to introduce an electric potential to realize electrolytic reduction.[236,237] As with chemical reduction, this idea is not commonly proposed for a *non-stoichiometric* oxide water splitting cycle and we are aware of only one report that validates the hypothesis. Recently, an experimental demonstration of the thermoelectrolytic reduction of CeO_2 in a CeO_2-YSZ composite achieved reduction temperatures as low as 850 °C with a 2 V applied potential, demonstrating H_2 productivity and complete oxidation reversibility.[238] The operating principles of electrolytic reduction are well known and studied in the field of solid-state ionics. In this process, the thermoelectrolytic cycle exploits the relatively large ionic and electronic conductivities of redox-active mixed ionic–electronic conducting oxides at elevated temperatures to effectively move oxygen ions and electrons through the material using an electrochemical

potential gradient that enables deep reduction at lower temperatures compared to thermal reduction. Preliminary thermodynamic analysis shows that when using concentrated solar irradiation as a heat input, coupled to electricity from photovoltaic cells, STH efficiency in excess of 30% is achievable. The process also offers a means to offset electrical requirements with process heat.[236,237] RD&D opportunities in this space exist for materials discovery and developing optimized electrochemical cells.

Integrated systems and TEA – upscaling, development, and commercialization of the TCH production pathway would greatly benefit by narrowing the TRL gap between the water splitting reactor (*i.e.*, the system that converts thermal energy to H_2) and the remaining system components that store thermal energy, recover and recycle thermal energy, separate and purify gases, and compress product gases for downstream delivery. The solar-powered H_2 production reactor is at TRL 4–5. However, other integral components needed to complete the system are at TRL 1–2 because of the extreme environments and unique operating conditions encountered in the two-step non-stoichiometric MO_x cycle. For example, ultra-high temperature thermal energy storage and heat transfer components are notional or lab-scaled,[239] and novel ideas for efficient separation of H_2 from excess steam,[240] or maintaining low O_2 partial pressure in reduction,[241] are just beginning to emerge. And while TCH systems have the potential to advantageously integrate with downstream synthesis processes for chemicals like ammonia, methanol, and sustainable aviation fuel, designs for optimal thermal integration and pressurized oxidation strategies capable of efficiently delivering H_2 or syngas directly to downstream synthesis platforms at required process conditions have not been reported.

TEA of full-scale, integrated systems would help identify prospective pathways to market,[242] expose and help address key gaps in our understanding of system integration strategies, and stimulate needed RD&D beyond the H_2 production reactor. However, since concepts for the aforementioned advanced system components are immature, an alternative computational framework for conducting TEA is used (see SI). This alternative approach separates the cost of energy, derived from a concentrating solar power plant, from that of the hydrogen conversion (HC) plant – whose system boundary starts with energy input from the solar radiation (SR) plant. This separation provides an opportunity to input the energy required to produce H_2 in multiple ways without having to redo the analysis, thus facilitating the exploration of a wide range of potential new configurations in future studies. Furthermore, costs for HC and SR are based entirely on material costs (like concrete and steel that are precisely known) with single multipliers to simplify TEA, as opposed to summing over individual components in a detailed though uncertain plant design as is traditionally done.[181,243] More importantly, material intensity and power density (see Table 4) scaled by reactor volume is used to calculate HC CAPEX establishing an explicit link between these two metrics in affecting system cost. Fig. 12 shows a waterfall chart for the levelized costs for H_2 production derived from this more simplistic approach. Formulating and

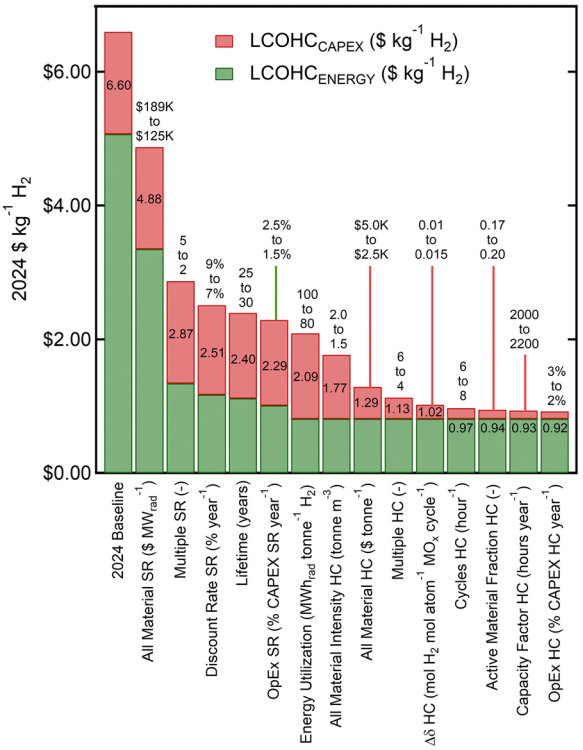

Fig. 12 Waterfall chart derived from TEA of a TCH process using methods described in this section. The cost of energy (LCOHC$_{ENERGY}$) dominates H_2 production cost in this example where a concentrating solar power plant (SR) provides thermal energy to the H_2 conversion process (HC). This analysis exposes a need to reduce SR material intensity and exploit novel heliostat field designs that decrease SR factors in order to achieve costs targets. Similarly, HC material costs that are determined by the metrics described in Table 4, and are influenced by scaling and learning, have a significant impact on breaking the \$2 kg^{-1} H_2 barrier.

understanding cost tradeoffs between choosing a lower performing material (reflected in the power density) if the system can be realized using a lower material intensity, relative to a competing concept, are easily visualized using this approach. As with other more traditional methods of TEA, single multipliers embody scaling, learning, land use, and operational factors that can be directly linked to and informed by a component-based approach. The chart in Fig. 12 is consistent with current thinking about how the cost of energy dominates the TCH technology landscape, and where design improvements that reduce material intensity for both SR and HC are needed to achieve ultimate cost targets.

Economics will ultimately define the success of TCH technologies. The levelized cost of hydrogen must be driven down by targeting the largest cost contributors with the discipline and foresight gained by developing a comprehensive technology development roadmap. Here, there is need and opportunity for the community to develop such a plan.

5. Closing remarks

Hydrogen production technologies based on PEC, BioH_2, and TCH water splitting represent three distinct but complementary

pathways toward a carbon-neutral, secure and resilient energy future. Each offers unique operational modalities and process architectures that collectively broaden the technological landscape for sustainable hydrogen generation. Importantly, these approaches do not converge on a singular, optimal solution, but rather open a suite of options that can be matched to geographic, economic, and infrastructural conditions. In so doing, they offer differentiating strategies to support the diversification and resilience embodied in the H2@Scale model.

Despite differences in scale, energy input, and feedstock compatibility, the PEC, BioH_2, and TCH platforms share a set of cross-cutting technical challenges that must be addressed to achieve cost-competitive, durable, and efficient systems. Central to all is the imperative to develop robust materials and operations capable of withstanding uniquely challenging and variable operating environments, including exposure to concentrated sunlight, high temperatures, feedstock variability, or reactive intermediates. Stability over prolonged operational cycles, resistance to fouling and degradation, and compatibility with system integration requirements remain critical barriers. The U.S. DOE BES has recognized that a deep mechanistic understanding of chemical reactions, interfacial phenomena, and materials transformations underpinning degradation phenomena at relevant operating conditions is needed to address these barriers.[244] For example, in PEC systems, light-driven catalysis involves complex interfacial charge dynamics and competing recombination pathways, where small changes in catalyst morphology or surface chemistry can significantly influence performance and stability. In BioH_2 configurations, understanding microbial metabolism and electrode-biofilm interactions under electrochemical stimulation enables the development of strains and materials tailored for high conversion efficiency and fouling resistance. TCH systems require detailed insight into redox thermodynamics, oxygen exchange kinetics, and sintering or phase segregation phenomena in metal oxide materials under thermal stress. Fundamental science plays an indispensable role in overcoming these challenges.

At the system level, engineering solutions must account for not only component optimization but also reactor integration, thermal management, gas separation, H_2 storage and transport, and process scalability. PEC systems must integrate light absorption across the solar spectrum and operate at low overpotentials to enable chemical conversion efficiency while maintaining compact, modular designs. They must also manage alternating on-and-off states and variable insolation over days and seasons. BioH_2 systems require innovations for process intensification, in reactor architecture as well as feedstock processing, that support continuous operation in spite of feedstock variability. TCH systems demand reactor designs capable of tolerating ultra-high temperatures and thermal cycling while maximizing solar energy capture and conversion efficiency. The importance of coupling materials and system design—through coordinated co-development—is increasingly recognized as essential to accelerate progress toward commercial readiness.

Importantly, these technologies serve distinct deployment contexts. PEC and BioH_2 systems offer promise for distributed, decentralized hydrogen production in regions lacking extensive energy infrastructure, enabling flexible integration into local energy systems or industrial processes. Their potential to utilize low-grade or waste inputs, such as wastewater, agricultural residues, or diffuse solar irradiation, supports circular economy principles and resource efficiency. Decentralized production places dispatchability in the forefront, so that H_2 can readily be moved to wherever it is needed. In contrast, TCH systems are inherently more centralized and thermally intensive, making them suitable for industrial-scale H_2 supply in regions with high solar direct normal irradiance and existing large-scale pipeline and chemical processing infrastructures able to take advantage of TCH's thermal integration potential. These differences in deployment scale and regional suitability emphasize the complementarity of the three pathways rather than competition, positioning them as mutually reinforcing elements within a diversified hydrogen production portfolio.

The path forward necessitates a coordinated research and development agenda that leverages advances in both fundamental science and engineering. Priorities include the development of multifunctional materials with high selectivity and durability, reactor systems that can maintain performance under fluctuating environmental and load conditions, and scalable architectures that minimize cost while maximizing H_2 yield. In parallel, continued innovation in modeling, simulation, and data-driven design will play a critical role in accelerating discovery and de-risking scale-up. Cross-platform learning, where advances in one pathway inform breakthroughs in another, offers a unique advantage in the development of complementary and adaptable hydrogen production solutions.

As global decarbonization goals intensify and renewable H_2 emerges as a central energy carrier, enabling a diverse set of production technologies becomes increasingly important. PEC, BioH_2, and TCH systems together offer a rich landscape of opportunity—spanning distributed and centralized scales, low- and high-temperature processes, and electrical, biological, and thermal energy inputs that by design are not strongly dependent on grid electricity. By advancing these platforms in parallel, the research community can ensure a resilient, context-sensitive hydrogen supply that meets the demands of H2@scale.

Author contributions

The authors CX, DE, DK, EW, FH, JM, PA, SH, SH, and YA contributed to development and writing of the Photoelectrochemical Hydrogen Pathway section, authors AB, AE, AM, BL, ES, HB, KC, LW, PM, RR, and TC contributed to development and writing of the Biological Hydrogen Pathway section, and authors AS, AL, CF, DG, ES, EK, GN, PL, and AM contributed to development and writing of the Thermochemical Hydrogen Pathway section. All authors attended the Technical Experts Meetings. KC, AM, and FH are corresponding authors and served as meeting co-chairs.

Conflicts of interest

There are no conflicts to declare.

Data availability

The data supporting this article have been included as part of the supplementary information. The file contains: definition of biohydrogen. Biohydrogen production from solid food waste. Microbial electrolysis cell properties. Data used to construct Fig. 5, 7, 8 and 12. Material usage and costs for solar thermochemical hydrogen generator. See DOI: https://doi.org/10.1039/d5ee04503g.

Acknowledgements

We gratefully acknowledge the Hydrogen and Fuel Cell Technologies Office (HFTO) and the Office of Basic Energy Sciences (BES) within the U.S. Department of Energy (U.S. DOE). Within HFTO specifically, authors are thankful for support from the HydroGEN Advanced Water Splitting Materials Consortium (part of the U.S. DOE Energy Materials Network) and the BioHydrogen Consortium, both established under the U.S. DOE, Office of Energy Efficiency and Renewable Energy (EERE). This article evolved from presentations and discussions at the workshop "Advanced Pathways Technical Experts Meeting" held in April 2024. Additional organizers of that workshop are Christina Vader, David Aguerrebere, Drs. Eric Miller, Viviane Schwartz, Victoria Distefano, Gail McLean, James Vickers, Katherine Rinaldi, and Kim Cierpik-Gold. Additional participants in that workshop are Drs. Huyen Dinh, Kathy Ayers, Yanfa Yan, Harvey Hou, Brian James, Bilge Yildiz, Jonathan Scheffe, Kevin Huang, Nicholas Strange, Chris Hahn, and Zetian Mi. We thank them for their contributions. In addition, KC gratefully acknowledges support provided by Southern California Gas Company under TSA-24-30976-0. KC, ASB, and HB also gratefully acknowledge Mohamad Jamal Abdallah for graphic support. YA acknowledges support from the U.S. DOE under Contract No. DE-EE0009629 with Strategic Analysis, Inc. Furthermore, this material is partially based on work performed by PA, FH, and EW under the Liquid Sunlight Alliance, which is supported by the U.S. DOE BES Fuels from Sunlight Hub under Award Number DE-SC0021266. AB gratefully acknowledges financial support from the Programa de Atracción de Talento of the Comunidad de Madrid (2020-T1/AMB-19884), the Consolidación Investigadora program of the Spanish State Research Agency (CNS2023-144887), and the COCREA program of CSIC (COCRE23009). DE acknowledges support from Ensembles of Photosynthetic Nanoreactors (EPN), an Energy Frontier Research Center (EFRC) funded by the U.S. DOE BES under Award no. DE-SC0023431. SH acknowledges funding by the Swiss National Science Foundation Sinergia grant #CRSII5_202225. SH gratefully acknowledges the U.S. DOE BES for the financial support provided by the Division of Chemical Sciences, Geosciences and Biosciences, through an Early Career grant No. DE-SC0021953, and by EERE under Award Number DE-EE0010734. DK was supported by the Center for Electrochemical Dynamics and Reactions on Surfaces (CEDARS), an EFRC funded by the U.S. DOE BES at the North Carolina A&T State University under Award Number DE-SC0023415. AL gratefully acknowledges research support from HFTO under Award Number DE-EE0008091. Work by GM was supported by the Center for Hybrid Approaches in Solar Energy to Liquid Fuels (CHASE), an Energy Innovation Hub funded by the U.S. DOE BES under Award Number DE-SC0021173. ES gratefully acknowledges research support from HFTO under Award Numbers DE-EE0010732 and DE-EE0010733. CX acknowledges support from HFTO under Contract Number WBS2.3.0.708. This work was authored [in part] by the National Laboratory of the Rockies for the U.S. DOE under Contract No. DE-AC36-08GO28308, and by Sandia National Laboratories, which is a multi-mission laboratory managed and operated by National Technology and Engineering Solutions of Sandia, LLC (NTESS), a wholly owned subsidiary of Honeywell International Inc., for the U.S. DOE's National Nuclear Security Administration (DOE/NNSA) under contract DE-NA0003525. This written work is authored by an employee of NTESS. The employee, not NTESS, owns the right, title and interest in and to the written work and is responsible for its contents. The views expressed in the article do not necessarily represent the views of the U.S. DOE or the U.S. Government. The U.S. Government retains and the publisher, by accepting the article for publication, acknowledges that the U.S. Government retains a nonexclusive, paid-up, irrevocable, worldwide license to publish or reproduce the published form of this work, or allow others to do so, for U.S. Government purposes.

Notes and references

1 B. Pivovar, N. Rustagi and S. Satyapal, *Electrochem. Soc. Interface*, 2018, **27**, 47–52.
2 *H2@Scale - a U.S. Department of Energy (DOE) initiative*, https://www.energy.gov/eere/fuelcells/h2scale, (accessed July 30, 2025).
3 M. Ruth, P. Jadun, N. Gilroy, E. Connelly, R. Boardman, A. J. Simon, A. Elgowainy and J. Zuboy, The Technical and Economic Potential of the H2@Scale Hydrogen Concept within the United States, *Report - NREL/TP-6A20-77610*, National Renewable Energy Laboratory, Golden, CO (United States), 2020.
4 *IEA, Global Hydrogen Review 2024, Report* https://www.iea.org/reports/global-hydrogen-review-2024, IEA, Paris, Fr, 2024.
5 M. Hubert, D. Peterson, E. Miller, J. Vickers, R. Mow and C. Howe, Clean Hydrogen Production Cost Scenarios with PEM Electrolyzer Technology, *Report from DOE Hydrogen Program Record #24005*, 2024.
6 S. R. Kurtz, A. Leilaeioun, R. R. King, I. M. Peters, M. J. Heben, W. K. Metzger and N. M. Haegel, *MRS Bull.*, 2020, **45**, 159–164.
7 E. Doyle and E. Krasowski, *Achieving affordable green hydrogen production plants, Ramboll*, https://www.ramboll.com/net-zero-explorers/what-will-it-take-to-reduce-capex-in-green-hydrogen-production, 2023.

8 M. H. Langholtz, D. Maggie, H. Chad, U. De La Torre, D. Efroymson, R. Jacobson, R. Milbrandt, A. Coleman, A. Davis, R. Kline, L. Keith, B. Alex, C. Scott, S. Erik, T. Timothy, F. Jeremy, E. Burton, L. Lixia, C. Hope, F. John, A. Robert, P. Esther, R. David, A. Karen, B. Craig, S. Troy, D. Kristen, O. Anne, C. Robin, M. Lee, C. Brandeis, C. Oyedeji, O. Klein, B. Wiatrowski, R. Matthew, H. Troy, O. Longwen, S. Udayan, Z. Jingyi, G. Song, S.-S. Lesley, V. Peter, X. Yiling, Z. Yunhua, J. De Angelo, N. Prakash, P. Jeffery, C. Kathleen, S. Benjamin, H. Eliza, O. Claire, C. Gregory, H. Jeffrey, S. Michael and W. Lee, 2023 Billion-Ton Report: An Assessment of U.S. Renewable Carbon Resources, 2024, DOI: 10.2172/2441098.

9 S. Alia, D. Ding, A. McDaniel, F. M. Toma and H. N. Dinh, *Electrochem. Soc.*, 2021, **30**, 50–56.

10 S. Ardo, D. F. Rivas, M. A. Modestino, V. S. Greiving, F. F. Abdi, E. Alarcon Llado, V. Artero, K. Ayers, C. Battaglia, J. P. Becker, D. Bederak, A. Berger, F. Buda, E. Chinello, B. Dam, V. Di Palma, T. Edvinsson, K. Fujii, H. Gardeniers, H. Geerlings, S. M. H. Hashemi, S. Haussener, F. Houle, J. Huskens, B. D. James, K. Konrad, A. Kudo, P. P. Kunturu, D. Lohse, B. Mei, E. L. Miller, G. F. Moore, J. Muller, K. L. Orchard, T. E. Rosser, F. H. Saadi, J. W. Schüttauf, B. Seger, S. W. Sheehan, W. A. Smith, J. Spurgeon, M. H. Tang, R. van de Krol, P. C. K. Vesborg and P. Westerik, *Energy Environ. Sci.*, 2018, **11**, 2768–2783.

11 B. A. Pinaud, J. D. Benck, L. C. Seitz, A. J. Forman, Z. B. Chen, T. G. Deutsch, B. D. James, K. N. Baum, G. N. Baum, S. Ardo, H. L. Wang, E. Miller and T. F. Jaramillo, *Energy Environ. Sci.*, 2013, **6**, 1983–2002.

12 C. X. Xiang, A. Z. Weber, S. Ardo, A. Berger, Y. K. Chen, R. Coridan, K. T. Fountaine, S. Haussener, S. Hu, R. Liu, N. S. Lewis, M. A. Modestino, M. M. Shaner, M. R. Singh, J. C. Stevens, K. Sun and K. Walczak, *Angew. Chem., Int. Ed.*, 2016, **55**, 12974–12988.

13 M. A. Modestino and S. Haussener, *Annu. Rev. Chem. Biomol.*, 2015, **6**, 13–34.

14 R. B. Chandran, S. Breen, Y. X. Shao, S. Ardo and A. Z. Weber, *Energy Environ. Sci.*, 2018, **11**, 115–135.

15 M. Dumortier, S. Tembhurne and S. Haussener, *Energy Environ. Sci.*, 2015, **8**, 3614–3628.

16 G. Segev, J. Kibsgaard, C. Hahn, Z. J. Xu, W. H. Cheng, T. G. Deutsch, C. X. Xiang, J. Z. Zhang, L. Hammarström, D. G. Nocera, A. Z. Weber, P. Agbo, T. Hisatomi, F. E. Osterloh, K. Domen, F. F. Abdi, S. Haussener, D. J. Miller, S. Ardo, P. C. McIntyre, T. Hannappel, S. Hu, H. Atwater, J. M. Gregoire, M. Z. Ertem, I. D. Sharp, K. S. Choi, J. S. Lee, O. Ishitani, J. W. Ager, R. R. Prabhakar, A. T. Bell, S. W. Boettcher, K. Vincent, K. Takanabe, V. Artero, R. Napier, B. Roldan Cuenya, M. T. M. Koper, R. Van de Krol and F. Houle, *J. Phys. D: Appl. Phys.*, 2022, **55**, ARTN 323003.

17 A. Cattry, H. Johnson, D. Chatzikiriakou and S. Haussener, *Energy Fuel*, 2024, **38**, 12058–12077.

18 A. Vilanova, P. Dias, T. Lopes and A. Mendes, *Chem. Soc. Rev.*, 2024, **53**, 2388–2434.

19 R. Sathre, J. B. Greenblatt, K. Walczak, I. D. Sharp, J. C. Stevens, J. W. Ager and F. A. Houle, *Energy Environ. Sci.*, 2016, **9**, 803–819.

20 R. Sathre, C. D. Scown, W. R. Morrow, J. C. Stevens, I. D. Sharp, J. W. Ager Iii, K. Walczak, F. A. Houle and J. Greenblatt, *Energy Environ. Sci.*, 2014, **7**, 3264–3278.

21 R. H. Coridan, A. C. Nielander, S. A. Francis, M. T. McDowell, V. Dix, S. M. Chatman and N. S. Lewis, *Energy Environ. Sci.*, 2015, **8**, 2886–2901.

22 I. Holmes-Gentle, S. Tembhurne, C. Suter and S. Haussener, *Nat. Energy*, 2023, **8**, 586–596.

23 Z. N. Song, C. W. Li, L. Chen, K. Dolia, S. Fu, N. N. Sun, Y. Li, K. Wyatt, J. L. Young, T. G. Deutsch and Y. F. Yan, *ACS Energy Lett.*, 2023, **8**, 2611–2619.

24 C. C. L. McCrory, S. Jung, I. M. Ferrer, S. M. Chatman, J. C. Peters and T. F. Jaramillo, *J. Am. Chem. Soc.*, 2015, **137**, 4347–4357.

25 B. D. James, D. A. DeSantis, J. M. Huya-Kouadio, C. Houchins, Y. Acevedo and G. Saur, *Hydrogen Production and Delivery Analysis*, 2021.

26 M. R. Shaner, H. A. Atwater, N. S. Lewis and E. W. McFarland, *Energy Environ. Sci.*, 2016, **9**, 2354–2371.

27 A. Grimm, W. A. de Jong and G. J. Kramer, *Int. J. Hydrogen Energy*, 2020, **45**, 22545–22555.

28 A. Sharma, T. Longden, K. Catchpole and F. J. Beck, *Energy Environ. Sci.*, 2023, **16**, 4486–4501.

29 C. Palmer, F. Saadi and E. W. McFarland, *ACS Sustainable Chem. Eng.*, 2018, **6**, 7003–7009.

30 T. A. Kistler, G. S. Zeng, J. L. Young, L. C. Weng, C. Aldridge, K. Wyatt, M. A. Steiner, O. Solorzano, F. A. Houle, F. M. Toma, A. Z. Weber, T. G. Deutsch and N. Danilovic, *Adv. Energy Mater.*, 2020, **10**, ARTN 2002706.

31 M. Ben-Naim, C. W. Aldridge, M. A. Steiner, A. C. Nielander, T. G. Deustch, J. L. Young and T. F. Jaramillo, *Chem. Catal.*, 2022, **2**, 195–209.

32 K. A. Walczak, G. Segev, D. M. Larson, J. W. Beeman, F. A. Houle and I. D. Sharp, *Adv. Energy Mater.*, 2017, 7.

33 H. Nishiyama, T. Yamada, M. Nakabayashi, Y. Maehara, M. Yamaguchi, Y. Kuromiya, Y. Nagatsuma, H. Tokudome, S. Akiyama, T. Watanabe, R. Narushima, S. Okunaka, N. Shibata, T. Takata, T. Hisatomi and K. Domen, *Nature*, 2021, **598**, 304.

34 H. Lyu, T. Hisatomi, Y. Goto, M. Yoshida, T. Higashi, M. Katayama, T. Takata, T. Minegishi, H. Nishiyama, T. Yamada, Y. Sakata, K. Asakura and K. Domen, *Chem. Sci.*, 2019, **10**, 3196–3201.

35 G. Heremans, C. Trompoukis, N. Daems, T. Bosserez, I. F. J. Vankelecom, J. A. Martens and J. Rongé, *Sustainable Energy Fuels*, 2017, **1**, 2061–2065.

36 M. N. Lee, S. Haas, V. Smirnov, T. Merdzhanova and U. Rau, *ChemElectroChem*, 2022, **9**, ARTN e202200838.

37 J. Y. Jia, L. C. Seitz, J. D. Benck, Y. J. Huo, Y. S. Chen, J. W. D. Ng, T. Bilir, J. S. Harris and T. F. Jaramillo, *Nat. Commun.*, 2016, **7**, ARTN 13237.

38 *U. DOE, Hydrogen Shot: Water Electrolysis Technology Assessment*, https://www.energy.gov/eere/fuelcells/hydrogen-shot-water-electrolysis-technology-assessment.
39 *VDMA, International Technology Roadmap for Photovoltaics (ITRPV)*, https://www.vdma.org/international-technology-roadmap-photovoltaic.
40 A. Heller, *Science*, 1984, **223**, 1141–1148.
41 H. Gerischer, *Pure Appl. Chem.*, 1980, **52**, 2649–2667.
42 S. Hu, M. R. Shaner, J. A. Beardslee, M. Lichterman, B. S. Brunschwig and N. S. Lewis, *Science*, 2014, **344**, 1005–1009.
43 T. A. Kistler, N. Danilovic and P. Agbo, *J. Electrochem. Soc.*, 2019, **166**, H656–H661.
44 T. A. Kistler, M. Y. Um and P. Agbo, *J. Electrochem. Soc.*, 2020, **167**, ARTN 066502.
45 D. M. Fabian, S. Hu, N. Singh, F. A. Houle, T. Hisatomi, K. Domen, F. E. Osterlohf and S. Ardo, *Energy Environ. Sci.*, 2015, **8**, 2825–2850.
46 T. Minegishi, N. Nishimura, J. Kubota and K. Domen, *Chem. Sci.*, 2013, **4**, 1120–1124.
47 Y. X. Wei, Z. Y. Zhang, W. J. Wang, Z. M. Song, M. D. Cai and S. Sun, *Chem. Phys. Chem.*, 2023, **24**, ARTN e202300216.
48 L. J. Guo, J. Z. Su, Z. Q. Wang, J. W. Shi, X. J. Guan, W. Cao and Z. S. Ou, *Int. J. Hydrogen Energy*, 2024, **51**, 1055–1078.
49 Q. Wang, T. Hisatomi, Q. X. Jia, H. Tokudome, M. Zhong, C. Z. Wang, Z. H. Pan, T. Takata, M. Nakabayashi, N. Shibata, Y. B. Li, I. D. Sharp, A. Kudo, T. Yamada and K. Domen, *Nat. Mater.*, 2016, **15**, 611.
50 M. Dumortier and S. Haussener, *Energy Environ. Sci.*, 2015, **8**, 3069–3082.
51 B. Tam, O. Babacan, A. Kafizas and J. Nelson, *Energy Environ. Sci.*, 2024, **17**, 1677–1694.
52 M. T. Spitler, M. A. Modestino, T. G. Deutsch, C. X. X. Xiang, J. R. Durrant, D. V. Esposito, S. Haussener, S. Maldonado, I. D. Sharp, B. A. Parkinson, D. S. Ginley, F. A. Houle, T. Hannappel, N. R. Neale, D. G. Nocera and P. C. McIntyre, *Sustainable Energy Fuels*, 2020, **4**, 985–995.
53 J. Albero, Y. Peng and H. García, *ACS Catal.*, 2020, **10**, 5734–5749.
54 J. L. White, M. F. Baruch, J. Pander, Y. Hu, I. C. Fortmeyer, J. E. Park, T. Zhang, K. Liao, J. Gu, Y. Yan, T. W. Shaw, E. Abelev and A. B. Bocarsly, *Chem. Rev.*, 2015, **115**, 12888–12935.
55 M. Ismael and M. Wark, *Appl. Mater. Today*, 2024, 39.
56 W. P. Yang, J. L. Wang, R. M. Chen, L. Xiao, S. J. Shen, J. Y. Li and F. Dong, *J. Mater. Chem. A*, 2022, **10**, 17357–17376.
57 Y. Xue, Y. T. Wang, Z. H. Pan and K. Sayama, *Angew. Chem., Int. Ed.*, 2021, **60**, 10469–10480.
58 Z. L. Wang, T. Hisatomi, R. G. Li, K. Sayama, G. Liu, K. Domen, C. Li and L. Z. Wang, *Joule*, 2021, **5**, 344–359.
59 M. F. Lagadec and A. Grimaud, *Nat. Mater.*, 2020, **19**, 1140.
60 *World Energy Outlook*, https://www.iea.org/reports/world-energy-outlook-2024, (accessed April 30, 2025).
61 J. C. W. Stevens and A. Z. Weber, *J. Electrochem. Soc.*, 2016, **163**, H475–H484.
62 A. Gupta, B. Likozar and S. Jaidka, *Renewable Sustainable Energy Rev.*, 2025, 208.
63 F. Nandjou and S. Haussener, *J. Phys. D: Appl. Phys.*, 2017, 50.
64 M. Ben-Naim, R. J. Britto, C. W. Aldridge, R. Mow, M. A. Steiner, A. C. Nielander, L. A. King, D. J. Friedman, T. G. Deutsch, J. L. Young and T. F. Jaramillo, *ACS Energy Lett.*, 2020, **5**, 2631–2640.
65 S. Hu, N. S. Lewis, J. W. Ager, J. H. Yang, J. R. McKone and N. C. Strandwitz, *J. Phys. Chem. C*, 2015, **119**, 24201–24228.
66 M. Xiao, Z. L. Wang, K. Maeda, G. Liu and L. Z. Wang, *Chem. Sci.*, 2023, **14**, 3415–3427.
67 B. Abhishek, A. Jayarama, A. S. Rao, S. S. Nagarkar, A. Dutta, S. P. Duttagupta, S. S. Prabhu and R. Pinto, *Int. J. Hydrogen Energy*, 2024, **81**, 1442–1466.
68 A. Karimi and J. L. Martin, *Int. Met. Rev.*, 1986, **31**, 1–26.
69 C. Tan, J. Shang and Z. Li, *Phys. Fluids*, 2024, 36.
70 P. C. Okonkwo, I. Ben Belgacem, W. Emori and P. C. Uzoma, *Int. J. Hydrogen Energy*, 2021, **46**, 27956–27973.
71 V. M. Ehlinger, A. Kusoglu and A. Z. Weber, *J. Electrochem. Soc.*, 2019, **166**, F3255–F3267.
72 J. Kibsgaard and I. Chorkendorff, *Nat. Energy*, 2019, **4**, 430–433.
73 P. von Tettau, P. Thiele, P. Mauermann, M. Wick, S. Tinz and S. Pischinger, *J. Power Sources*, 2025, 630.
74 L. Barrera, B. W. Layne, Z. J. Chen, K. Watanabe, A. Kudo, D. V. Esposito, S. Ardo and R. B. Chandran, *Energy Environ. Sci.*, 2024, **17**, 8254–8273.
75 P. Zhou, I. A. Navid, Y. J. Ma, Y. X. Xiao, P. Wang, Z. W. Ye, B. W. Zhou, K. Sun and Z. T. Mi, *Nature*, 2023, **613**, 66.
76 Y. Ma, X. L. Wang, Y. S. Jia, X. B. Chen, H. X. Han and C. Li, *Chem. Rev.*, 2014, **114**, 9987–10043.
77 J. Suntivich, G. Hautier, I. Dabo, E. J. Crumlin, D. Kumar and T. Cuk, *Nat. Energy*, 2024, **9**, 1191–1198.
78 N. R. Mucha, J. Som, J. Choi, S. Shaji, R. K. Gupta, H. M. Meyer, C. L. Cramer, A. M. Elliott and D. Kumar, *ACS Appl. Energy Mater.*, 2020, **3**, 8366–8374.
79 J. A. Lin, I. Roh and P. D. Yang, *J. Am. Chem. Soc.*, 2023, **145**, 12987–12991.
80 Z. G. Schichtl, S. K. Conlin, H. Mehrabi, A. C. Nielander and R. H. Coridan, *ACS Appl. Energy Mater.*, 2022, **5**, 3863–3875.
81 T. A. Kistler, M. Y. Um, J. K. Cooper, I. D. Sharp and P. Agbo, *Energy Environ. Sci.*, 2022, **15**, 2061–2070.
82 S. Tembhurne and S. Haussener, *J. Electrochem. Soc.*, 2016, **163**, H999–H1007.
83 T. Y. Liu, P. Wang, W. Li, D. Z. Wang, D. D. Lekamge, B. Q. Chen, F. A. Houle, M. M. Waegele and D. W. Wang, *ACS Central Sci.*, 2024, **11**, 91–97.
84 Y. Y. Li, H. Zhou, S. H. Cai, D. Prabhakaran, W. T. Niu, A. Large, G. Held, R. A. Taylor, X. P. Wu and S. C. E. Tsang, *Nat. Catal.*, 2024, **7**, 77–88.
85 S. Collins, Y. Acevedo, D. V. Esposito, R. B. Chandran, S. Ardo, B. D. James and H. Breunig, *Energy Environ. Sci.*, 2025, **18**, 6690–6700.

86 H. Döscher, J. L. Young, J. F. Geisz, J. A. Turner and T. G. Deutsch, *Energy Environ. Sci.*, 2016, **9**, 74–80.
87 O. J. Alley, K. Wyatt, M. A. Steiner, G. J. Liu, T. Kistler, G. S. Zeng, D. M. Larson, J. K. Cooper, J. L. Young, T. G. Deutsch and F. M. Toma, *Front. Energy Res.*, 2022, 10.
88 S. Vanka, G. S. Zeng, T. G. Deutsch, F. M. Toma and Z. T. Mi, *Front. Energy Res.*, 2022, 10.
89 X. Shen, R. Yanagi, D. Solanki, H. Q. Su, Z. H. Li, C. X. Xiang and S. Hu, *Front. Energy Res.*, 2022, 9.
90 D. S. Ellis, Y. Piekner, D. A. Grave, P. Schnell and A. Rothschild, *Front. Energy Res.*, 2022, **9**, ARTN 726069.
91 H. Gaffron and J. Rubin, *J. Gen. Physiol.*, 1942, **26**, 219–240.
92 S. Lien and A. San Pietro, *Inquiry into biophotolysis of water to produce hydrogen, Indiana Univ., Bloomington (USA)*, Dept. of Plant Sciences, United States, 1976.
93 P. F. Weaver, S. Lien and M. Seibert, *Sol. Energy*, 1980, **24**, 3–45.
94 A. Melis, L. Zhang, M. Forestier, M. L. Ghirardi and M. Seibert, *Plant Physiol.*, 2000, **122**, 127–136.
95 E. Touloupakis, C. Faraloni, A. M. Silva Benavides and G. Torzillo, *Energies*, 2021, **14**, 7170.
96 X. Gómez, M. J. Cuetos, J. I. Prieto and A. Morán, *Renewable Energy*, 2009, **34**, 970–975.
97 A. Singh, S. Sevda, I. M. Abu Reesh, K. Vanbroekhoven, D. Rathore and D. Pant, *Energies*, 2015, **8**, 13062–13080.
98 C.-L. Cheng, Y.-C. Lo, K.-S. Lee, D.-J. Lee, C.-Y. Lin and J.-S. Chang, *Bioresour. Technol.*, 2011, **102**, 8514–8523.
99 I. K. Kapdan and F. Kargi, *Enzyme Microb. Technol.*, 2006, **38**, 569–582.
100 J. J. Alvarado-Flores, J. V. Alcaraz-Vera, M. L. Ávalos-Rodríguez, E. Guzmán-Mejía, J. G. Rutiaga-Quiñones, L. F. Pintor-Ibarra and S. J. Guevara-Martínez, *Energies*, 2024, **17**, 537.
101 G. Maitlo, I. Ali, K. H. Mangi, S. Ali, H. A. Maitlo, I. N. Unar and A. M. Pirzada, *Sustainability*, 2022, **14**, 2596.
102 B. E. Logan, B. Hamelers, R. Rozendal, U. Schröder, J. Keller, S. Freguia, P. Aelterman, W. Verstraete and K. Rabaey, *Environ. Sci. Technol.*, 2006, **40**, 5181–5192.
103 S. Cheng and B. E. Logan, *Proc. Natl. Acad. Sci. U. S. A.*, 2007, **104**, 18871–18873.
104 E. Lalaurette, S. Thammannagowda, A. Mohagheghi, P.-C. Maness and B. E. Logan, *Int. J. Hydrogen Energy*, 2009, **34**, 6201–6210.
105 S. Venkata Mohan and A. Pandey, in *Biohydrogen*, ed A. Pandey, S. V. Mohan, J.-S. Chang, P. C. Hallenbeck and C. Larroche, Elsevier, 2nd edn, 2019, pp. 1–23, DOI: 10.1016/B978-0-444-64203-5.00001-0.
106 R. Kumar, A. Kumar and A. Pal, *Int. J. Hydrogen Energy*, 2022, **47**, 34831–34855.
107 D. B. Levin, L. Pitt and M. Love, *Int. J. Hydrogen Energy*, 2004, **29**, 173–185.
108 Y. Lou, Z. Fan, J. Friedmann, A.-S. Corbeau, M. Agrawal and A. Khatri, The Potential Role of Biohydrogen in Creating a Net-Zero World; The Production and Applications of Carbon-Negative Hydrogen, 2023.
109 M. L. Ghirardi, A. Dubini, J. Yu and P. C. Maness, *Chem. Soc. Rev.*, 2009, **38**, 52–61.
110 J. Turner, G. Sverdrup, M. K. Mann, P.-C. Maness, B. Kroposki, M. Ghirardi, R. J. Evans and D. Blake, *Int. J. Energy Res.*, 2008, **32**, 379–407.
111 Q. Zhang, in *Waste to Renewable Biohydrogen*, ed Q. Zhang, C. He, J. Ren and M. Goodsite, Academic Press, 2021, pp. 55–70, DOI: 10.1016/B978-0-12-821659-0.00002-2.
112 S. F. Ahmed, N. Rafa, M. Mofijur, I. A. Badruddin, A. Inayat, M. S. Ali, O. Farrok and T. M. Yunus Khan, *Front. Energy Res.*, 2021, **9**, 753878.
113 V. Ananthi, A. Bora, U. Ramesh, R. Yuvakkumar, K. Raja, K. Ponnuchamy, G. Muthusamy and A. Arun, *Process Saf. Environ. Prot.*, 2024, **186**, 944–956.
114 K. J. Chou, T. Croft, S. D. Hebdon, L. R. Magnusson, W. Xiong, L. H. Reyes, X. Chen, E. J. Miller, D. M. Riley, S. Dupuis, K. A. Laramore, L. M. Keller, D. Winkelman and P. C. Maness, *Metab. Eng.*, 2024, **83**, 193–205.
115 D. P. Clark, *FEMS Microbiol. Rev.*, 1989, **5**, 223–234.
116 A. L. Demain, M. Newcomb and J. D. Wu, *Microbiol. Mol. Biol. Rev.*, 2005, **69**, 124–154.
117 Y. Lin, M. Roni, D. S. Hartley, P. H. Burli, D. N. Thompson and L. Ou, *Herbaceous Feedstock 2022 State of Technology Report*, United States, 2024.
118 R. Rossi, J. Nicolas and B. E. Logan, *J. Power Sources*, 2023, **560**, 232594.
119 D. Kim, N. Yun, H. Du, D. A. Moreno Jimenez and R. Rossi, *J. Power Sources*, 2025, **630**, 236077.
120 A. B. Xinyu Liu, A. Elgowainy, K. J. Chou, A. Beliaev, E. Hill, S. W. Singer and E. Sundstrom, *2022 AIChE Annual Meeting*, 2022.
121 M. M. Albuquerque, G. d B. Sartor, W. J. Martinez-Burgos, T. Scapini, T. Edwiges, C. R. Soccol and A. B. P. Medeiros, *Methane*, 2024, **3**, 500–532.
122 A. Ahmad, K. Rambabu, S. W. Hasan, P. L. Show and F. Banat, *Int. J. Hydrogen Energy*, 2024, **52**, 335–357.
123 I. W. Changman Kim, C. Dou, L. Magnusson, P.-C. Maness, K. J. Chou, S. Singer and E. Sundstrom, *Chem. Eng. J.*, 2023, **456**, 141028.
124 L. R. Lynd, P. J. Weimer, W. H. van Zyl and I. S. Pretorius, *Microbiol. Mol. Biol. Rev.*, 2002, **66**, 506–577.
125 F. R. Hawkes, I. Hussy, G. Kyazze, R. Dinsdale and D. L. Hawkes, *Int. J. Hydrogen Energy*, 2007, **32**, 172–184.
126 G. Sołowski, I. Konkol and A. Cenian, *J. Cleaner Prod.*, 2020, **267**, 121721.
127 E. K. Holwerda, P. G. Thorne, D. G. Olson, D. Amador-Noguez, N. L. Engle, T. J. Tschaplinski, J. P. van Dijken and L. R. Lynd, *Biotechnol. Biofuels*, 2014, **7**, 155.
128 M. Cha, D. Chung, J. G. Elkins, A. M. Guss and J. Westpheling, *Biotechnol. Biofuels*, 2013, **6**, 85.
129 J. Lo, T. Zheng, D. G. Olson, N. Ruppertsberger, S. A. Tripathi, L. Tian, A. M. Guss and L. R. Lynd, *J. Bacteriol.*, 2015, **197**, 2920–2929.
130 B. Tunca, F. E. Kutlar, A. Kas and Y. D. Yilmazel, *Waste Manage.*, 2023, **171**, 401–410.

131 T. J. Verbeke, G. M. Garcia and J. G. Elkins, *Biotechnol. Biofuels*, 2017, **10**, 233.
132 X. Shao, S. J. Murphy and L. R. Lynd, *Biomass Bioenergy*, 2020, **139**, 105623.
133 M. R. Kubis, E. K. Holwerda and L. R. Lynd, *Biotechnol. Biofuels Bioprod.*, 2022, **15**, 12.
134 D. Beri, C. D. Herring, S. Blahova, S. Poudel, R. J. Giannone, R. L. Hettich and L. R. Lynd, *Biotechnol. Biofuels*, 2021, **14**, 24.
135 R. G. Bing, M. J. Carey, T. Laemthong, D. J. Willard, J. R. Crosby, D. B. Sulis, J. P. Wang, M. W. W. Adams and R. M. Kelly, *Bioresour. Technol.*, 2023, **367**, 128275.
136 M. Basen, A. M. Rhaesa, I. Kataeva, C. J. Prybol, I. M. Scott, F. L. Poole and M. W. Adams, *Bioresour. Technol.*, 2014, **152**, 384–392.
137 M. R. Kubis, E. K. Holwerda and L. R. Lynd, *Biotechnol. Biofuels Bioprod.*, 2022, **15**, 12.
138 Y. Yin, W. Song and J. Wang, *Bioresour. Technol.*, 2022, **364**, 128074.
139 S. Larsson, E. Palmqvist, B. Hahn-Hägerdal, C. Tengborg, K. Stenberg, G. Zacchi and N.-O. Nilvebrant, *Enzyme Microb. Technol.*, 1999, **24**, 151–159.
140 P. C. López, C. Peng, N. Arneborg, H. Junicke and K. V. Gernaey, *Sci. Rep.*, 2021, **11**, 6853.
141 D. Nagarajan, D.-J. Lee and J.-S. Chang, *Int. J. Hydrogen Energy*, 2019, **44**, 14362–14379.
142 F.-M. Lin, B. Qiao and Y.-J. Yuan, *Appl. Environ. Microbiol.*, 2009, **75**, 3765–3776.
143 C. Janzowski, V. Glaab, E. Samimi, J. Schlatter and G. Eisenbrand, *Food Chem. Toxicol.*, 2000, **38**, 801–809.
144 T. J. Verbeke, R. J. Giannone, D. M. Klingeman, N. L. Engle, T. Rydzak, A. M. Guss, T. J. Tschaplinski, S. D. Brown, R. L. Hettich and J. G. Elkins, *Sci. Rep.*, 2017, **7**, 43355.
145 C. R. Carere, T. Rydzak, T. J. Verbeke, N. Cicek, D. B. Levin and R. Sparling, *BMC Microbiol.*, 2012, **12**, 295.
146 M. H. Langholtz, 2024, DOI: 10.23720/BT2023/2316165.
147 P. Lamers, M. S. Roni, J. S. Tumuluru, J. J. Jacobson, K. G. Cafferty, J. K. Hansen, K. Kenney, F. Teymouri and B. Bals, *Bioresour. Technol.*, 2015, **194**, 205–213.
148 *Feedstock Conversion Interface Conversion Capstone Report, Report DOE/EE-2956*, 2024.
149 Z. Li, H. Zhai, Y. Zhang and L. Yu, *Ind. Crops Prod.*, 2012, **37**, 130–136.
150 A. Ghimire, E. Trably, L. Frunzo, F. Pirozzi, P. N. L. Lens, G. Esposito, E. A. Cazier and R. Escudié, *Bioresour. Technol.*, 2018, **248**, 180–186.
151 C. Kim, I. Wolf, C. Dou, L. Magnusson, P.-C. Maness, K. J. Chou, S. Singer and E. Sundstrom, *Chem. Eng. J.*, 2023, **456**, 141028.
152 X. Wang, J. Ding, W.-Q. Guo and N.-Q. Ren, *Int. J. Hydrogen Energy*, 2010, **35**, 10960–10966.
153 A. D. N. F. J. Adriana, F. M. Braga and M. Zaiat, *J. Chem. Technol. Biotechnol.*, 2015, **91**, 967–976.
154 R. Kanniah Goud, K. Arunasri, D. K. Yeruva, K. V. Krishna, S. Dahiya and S. V. Mohan, *Bioresour. Technol.*, 2017, **242**, 253–264.
155 L. Magnusson, N. Cicek, R. Sparling and D. Levin, *Biotechnol. Bioeng.*, 2009, **102**, 759–766.
156 M. M. I. Anoy, E. A. Hill, M. R. Garcia, W.-J. Kim, A. S. Beliaev and H. Beyenal, *Enzyme Microb. Technol.*, 2024, **180**, 110502.
157 J. Jiang, J. A. Lopez-Ruiz, Y. Bian, D. Sun, Y. Yan, X. Chen, J. Zhu, H. D. May and Z. J. Ren, *Water Res.*, 2023, **241**, 120139.
158 L. Wang, K. Linowski and H. Liu, *Chem. Eng. J.*, 2023, **454**, 140257.
159 J. Li, Q. Wang and J. Zhang, *J. Power Sources*, 2024, **591**, 233855.
160 S. C. Popat and C. I. Torres, *Bioresour. Technol.*, 2016, **215**, 265–273.
161 C. I. Torres, A. Kato Marcus and B. E. Rittmann, *Biotechnol. Bioeng.*, 2008, **100**, 872–881.
162 P. Srivastava, E. García-Quismondo, J. Palma and C. González-Fernández, *Int. J. Hydrogen Energy*, 2024, **52**, 223–239.
163 A. Miller, L. Singh, L. Wang and H. Liu, *Environ. Int.*, 2019, **126**, 611–618.
164 R. Rossi, B. P. Cario, C. Santoro, W. Yang, P. E. Saikaly and B. E. Logan, *Environ. Sci. Technol.*, 2019, **53**, 3977–3986.
165 R. Rossi, D. Jones, J. Myung, E. Zikmund, W. Yang, Y. A. Gallego, D. Pant, P. J. Evans, M. A. Page, D. M. Cropek and B. E. Logan, *Water Res.*, 2019, **148**, 51–59.
166 L. C. Brown, G. Besenbruch, K. Schultz, S. Showalter, A. Marshall, P. Pickard and J. Funk, *High efficiency generation of hydrogen fuels using thermochemical cycles and nuclear power, Report GA–A24326*, 2002.
167 A. Steinfeld, *Sol. Energy*, 2005, **78**, 603–615.
168 S. Abanades, P. Charvin, G. Flamant and P. Neveu, *Energy*, 2006, **31**, 2805–2822.
169 C. Agrafiotis, M. Roeb and C. Sattler, *Renewable Sustainable Energy Rev.*, 2015, **42**, 254–285.
170 E. Koepf, I. Alxneit, C. Wieckert and A. Meier, *Appl. Energy*, 2017, **188**, 620–651.
171 F. Safari and I. Dincer, *Energy Convers. Manage.*, 2020, **205**, 112182.
172 S. Docao, A. R. Koirala, M. G. Kim, I. C. Hwang, M. K. Song and K. B. Yoon, *Energy Environ. Sci.*, 2017, **10**, 628–640.
173 D. Guban, I. K. Muritala, M. Roeb and C. Sattler, *Int. J. Hydrogen Energy*, 2020, **45**, 26156–26165.
174 E. Koepf, W. Villasmil and A. Meier, *Appl. Energy*, 2016, **165**, 1004–1023.
175 R. Perret, Solar Thermochemical Hydrogen Production Research (STCH) Thermochemical Cycle Selection and Investment Priority, *Report SAND2011-1141P, Sandia National Lab.(SNL-CA)*, Livermore, CA (United States), 2011.
176 Y. Lu, L. Zhu, C. Agrafiotis, J. Vieten, M. Roeb and C. Sattler, *Prog. Energy Combust. Sci.*, 2019, 75.
177 E. Alonso and M. Romero, *Renewable Sustainable Energy Rev.*, 2015, **41**, 53–67.
178 R. Schappi, D. Rutz, F. Dahler, A. Muroyama, P. Haueter, J. Lilliestam, A. Patt, P. Furler and A. Steinfeld, *Nature*, 2022, **601**, 63–68.

179 A. Lidor and B. Bulfin, *Solar Compass*, 2024, 11.
180 D. Marxer, P. Furler, M. Takacs and A. Steinfeld, *Energy Environ. Sci.*, 2017, **10**, 1142–1149.
181 V. K. Budama, N. G. Johnson, I. Ermanoski and E. B. Stechel, *Int. J. Hydrogen Energy*, 2021, **46**, 1656–1670.
182 J. Hinkley, J. Hayward, R. McNaughton, J. Edwards and K. Lovegrove, *Concentrating Solar Fuels Roadmap: Final Report*, CSIRO, Australia, 2016.
183 W.-H. Cheng, A. de la Calle, H. A. Atwater, E. B. Stechel and C. Xiang, *ACS Energy Lett.*, 2021, **6**, 3096–3113.
184 A. González-Pardo, T. Denk and A. Vidal, *AIP Conf. Proc.*, 2020, 2303.
185 V. K. Thanda, T. Fend, D. Laaber, A. Lidor, H. von Storch, J. P. Säck, J. Hertel, J. Lampe, S. Menz, G. Piesche, S. Berger, S. Lorentzou, M. Syrigou, T. Denk, A. Gonzales-Pardo, A. Vidal, M. Roeb and C. Sattler, *Renewable Energy*, 2022, **198**, 389–398.
186 *Hydrosol-BEYOND Consortium*, https://www.hydrosol-beyond.certh.gr/, (accessed February 18, 2025).
187 E. Koepf, S. Zoller, S. Luque, M. Thelen, S. Brendelberger, J. González-Aguilar, M. Romero and A. Steinfeld, Liquid fuels from concentrated sunlight: An overview on development and integration of a 50 kW solar thermochemical reactor and high concentration solar field for the SUN-to-LIQUID project, AIP Conference Proceedings, 2019, vol. 2126, ARTN 180012.
188 S. Zoller, E. Koepf, D. Nizamian, M. Stephan, A. Patane, P. Haueter, M. Romero, J. Gonzalez-Aguilar, D. Lieftink, W. E. De, S. Brendelberger, A. Sizmann and A. Steinfeld, *Joule*, 2022, **6**, 1606–1616.
189 S. Zoller, E. Koepf, P. Roos and A. Steinfeld, *J. Sol. Energy Eng.*, 2019, **141**, 021014.
190 *Sun-to-Liquid II*, https://sun-to-liquid-2.eu, (accessed July, 2025).
191 R. J. Carrillo and J. R. Scheffe, *Sol. Energy*, 2017, **156**, 3–20.
192 R. R. Bhosale, *Energies*, 2023, 16.
193 R. R. Bhosale, G. Takalkar, P. Sutar, A. Kumar, F. AlMomani and M. Khraisheh, *Int. J. Hydrogen Energy*, 2019, **44**, 34–60.
194 S. Abanades and G. Flamant, *Sol. Energy*, 2006, **80**, 1611–1623.
195 W. C. Chueh, C. Falter, M. Abbott, D. Scipio, P. Furler, S. M. Haile and A. Steinfeld, *Science*, 2010, **330**, 1797–1801.
196 A. Bayon, A. de la Calle, E. B. Stechel and C. Muhich, *Energy Technol.*, 2021, 10.
197 R. Schmitt, A. Nenning, O. Kraynis, R. Korobko, A. I. Frenkel, I. Lubomirsky, S. M. Haile and J. L. M. Rupp, *Chem. Soc. Rev.*, 2020, **49**, 554–592.
198 B. Baldassarri, J. He and C. Wolverton, *Phys. Rev. Mater.*, 2024, **8**, 055407.
199 S. Lany, *J. Chem. Phys.*, 2018, 148.
200 S. Lany, *J. Am. Chem. Soc.*, 2024, **146**, 14114–14127.
201 S. S. Naghavi, A. A. Emery, H. A. Hansen, F. Zhou, V. Ozolins and C. Wolverton, *Nat. Commun.*, 2017, 8.
202 A. de la Calle and A. Bayon, *Int. J. Hydrogen Energy*, 2019, **44**, 1409–1424.
203 A. Lidor, Y. Aschwanden, J. Häseli, P. Reckinger, P. Haueter and A. Steinfeld, *Appl. Energy*, 2023, 329.
204 A. Lidor and L. Zimmermann, *Sol. Energy*, 2023, 262.
205 A. de la Calle, I. Ermanoski, J. E. Miller and E. B. Stechel, *Int. J. Hydrogen Energy*, 2024, **72**, 1159–1168.
206 S. Li, V. M. Wheeler, P. B. Kreider and W. Lipinski, *Energy Fuel*, 2018, **32**, 10838–10847.
207 R. B. Diver, J. E. Miller, N. P. Siegel and T. A. Moss, *Es2010: Proceedings of Asme 4th International Conference on Energy Sustainability*, Vol 2, 2010, 97–104.
208 J. E. Miller, M. D. Allendorf, A. Ambrosini, E. N. Coker, R. B. Diver, I. Ermanoski, L. R. Evans, R. E. Hogan and A. McDaniel, *Development and assessment of solar-thermal-activated fuel production. Phase 1, summary, Report SAND2012-5658*, 2012.
209 N. P. Siegel, J. E. Miller, I. Ermanoski, R. B. Diver and E. B. Stechel, *Ind. Eng. Chem. Res.*, 2013, **52**, 3276–3286.
210 G. Ambrosetti and P. Good, *Sol. Energy*, 2019, **183**, 521–531.
211 O. A. Marina, Benchmarking, Protocol Development and Community Engagement of Advanced Water Splitting Technologies, Project ID # P170, https://www.hydrogen.energy.gov/docs/hydrogenprogramlibraries/pdfs/review24/p170_marina_2024_o.pdf?sfvrsn=96514c31_5, (accessed February 20, 2025).
212 H. Dinh, *HydroGEN Overview: A Consortium on Advanced Water Splitting Materials, Project ID # P148, pg. 60*, https://www.hydrogen.energy.gov/docs/hydrogenprogramlibraries/pdfs/review24/p148_dinh_2024_o.pdf?sfvrsn=74c04ea9_5, (accessed February 20, 2025).
213 J. E. Miller, A. H. McDaniel and M. D. Allendorf, *Adv. Energy Mater.*, 2013, 4.
214 D. R. Barcellos, M. D. Sanders, J. Tong, A. H. McDaniel and R. P. O'Hayre, *Energy Environ. Sci.*, 2018, **11**, 3256–3265.
215 *HydroGEN Advanced Water Splitting Materials Consortium*, https://www.energy.gov/eere/h2awsm/hydrogen-advanced-water-splitting-materials-consortium, (accessed February, 2025).
216 C. Falter, V. Batteiger and A. Sizmann, *Environ. Sci. Technol.*, 2016, **50**, 470–477.
217 O. Y. Long, G. S. Gautam and E. A. Carter, *Phys. Rev. Mater.*, 2020, **4**, ARTN 045401.
218 R. B. Wexler, G. S. Gautam, E. B. Stechel and E. A. Carter, *J. Am. Chem. Soc.*, 2021, **143**, 13212–13227.
219 A. Bayon, A. de la Calle, K. K. Ghose, A. Page and R. McNaughton, *Int. J. Hydrogen Energy*, 2020, **45**, 12653–12679.
220 B. Chen, H. Yang, Q. Dong, L. Tong, Y. Ding and L. Wang, *Int. J. Hydrogen Energy*, 2024, **84**, 1058–1067.
221 A. H. McDaniel, E. C. Miller, D. Arifin, A. Ambrosini, E. N. Coker, R. O'Hayre, W. C. Chueh and J. Tong, *Energy Environ. Sci.*, 2013, 6.
222 B. Meredig and C. Wolverton, *Phys. Rev. B: Condens. Matter Mater. Phys.*, 2009, 80.
223 B. Meredig and C. Wolverton, *Phys. Rev. B: Condens. Matter Mater. Phys.*, 2011, 83.
224 M. D. Witman, A. Goyal, T. Ogitsu, A. H. McDaniel and S. Lany, *Nat Comput Sci*, 2023, **3**, 675–686.

225 T. Xie and J. C. Grossman, *Phys. Rev. Lett.*, 2018, 120.
226 R. B. Wexler, G. Sai Gautam, R. T. Bell, S. Shulda, N. A. Strange, J. A. Trindell, J. D. Sugar, E. Nygren, S. Sainio, A. H. McDaniel, D. Ginley, E. A. Carter and E. B. Stechel, *Energy Environ. Sci.*, 2023, **16**, 2550–2560.
227 P. Furler, J. Scheffe, D. Marxer, M. Gorbar, A. Bonk, U. Vogt and A. Steinfeld, *Phys. Chem. Chem. Phys.*, 2014, **16**, 10503–10511.
228 A. Haeussler, S. Abanades, A. Julbe, J. Jouannaux and B. Cartoixa, *Energy*, 2020, **201**, ARTN 117649.
229 S. Sas Brunser, F. L. Bargardi, R. Libanori, N. Kaufmann, H. Braun, A. Steinfeld and A. R. Studart, *Adv. Mater. Interfaces*, 2023, **10**, ARTN 2300452.
230 F. A. Costa Oliveira, M. A. Barreiros, M. Sardinha, M. Leite, J. C. Fernandes and S. Abanades, *Int. J. Hydrogen Energy*, 2025, **100**, 477–490.
231 M. M. Nair and S. Abanades, *Energ Fuel*, 2016, **30**, 6050–6058.
232 K. Otsuka, Y. Wang, E. Sunada and I. Yamanaka, *J. Catal.*, 1998, **175**, 152–160.
233 P. T. Krenzke and J. H. Davidson, *Energy Fuel*, 2014, **28**, 4088–4095.
234 P. Ebrahimi, A. Kumar and M. Khraisheh, *Emergent Mater.*, 2020, **3**, 881–917.
235 N. Hajjaji, S. Martinez, E. Trably, J.-P. Steyer and A. Helias, *Int. J. Hydrogen Energy*, 2016, **41**, 6064–6075.
236 J. Perry, T. W. Jones, J. M. Coronado, S. W. Donne and A. Bayon, *Energy*, 2023, **276**, ARTN 127412.
237 G. L. Schieber, E. B. Stechel, A. Ambrosini, J. E. Miller and P. G. Loutzenhiser, *Int. J. Hydrogen Energy*, 2017, **42**, 18785–18793.
238 J. Perry, A. de la Calle, T. W. Jones, S. W. Donne, J. M. Coronado and A. Bayon, *Int. J. Hydrogen Energy*, 2025, **141**, 1172–1181.
239 A. Ramos, E. López, C. del Cañizo and A. Datas, *J Energy Storage*, 2022, **49**, ARTN 104131.
240 A. Lidor, *Int. J. Hydrogen Energy*, 2024, **94**, 664–668.
241 S. Brendelberger, H. von Storch, B. Bulfin and C. Sattler, *Sol. Energy*, 2017, **141**, 91–102.
242 G. J. Nathan, L. Lee, P. ingenhoven, Z. Tian, Z. Sun, A. Chinnici, M. Jafarian, P. Ashman, D. Potter and W. Saw, *Solar Compass*, 2017, **5**, 100036.
243 V. K. Budama, N. G. Johnson, A. McDaniel, I. Ermanoski and E. B. Stechel, *Int. J. Hydrogen Energy*, 2018, **43**, 17574–17587.
244 M. Bullock and K. More, *Basic Energy Sciences Roundtable: Foundational Science for Carbon-Neutral Hydrogen Technologies, Report OSTI ID: 1834317*, USDOE Office of Science (SC), Basic Energy Sciences (BES), 2021, DOI: 10.2172/1834317.